Exome-Derived Adiponectin-Associated Variants Implicate Obesity and Lipid Biology

Cassandra N. Spracklen,[1,91] Tugce Karaderi,[2,3,4,5,91] Hanieh Yaghootkar,[6,7] Claudia Schurmann,[8] Rebecca S. Fine,[9,10,11] Zoltan Kutalik,[6,12,13] Michael H. Preuss,[8] Yingchang Lu,[8,14,15] Laura B.L. Wittemans,[2,16] Linda S. Adair,[17] Matthew Allison,[18] Najaf Amin,[19] Paul L. Auer,[20] Traci M. Bartz,[21,22] Matthias Blüher,[23] Michael Boehnke,[24] Judith B. Borja,[25,26] Jette Bork-Jensen,[27] Linda Broer,[28] Daniel I. Chasman,[29,30] Yii-Der Ida Chen,[31] Paraskevi Chirstofidou,[32] Ayse Demirkan,[19] Cornelia M. van Duijn,[19] Mary F. Feitosa,[33] Melissa E. Garcia,[34] Mariaelisa Graff,[35,36] Harald Grallert,[37,38] Niels Grarup,[27] Xiuqing Guo,[31] Jeffrey Haesser,[39] Torben Hansen,[27] Tamara B. Harris,[40] Heather M. Highland,[35] Jaeyoung Hong,[41] M. Arfan Ikram,[28,42] Erik Ingelsson,[43,44,45,46] Rebecca Jackson,[47] Pekka Jousilahti,[48] Mika Kähönen,[49,50] Jorge R. Kizer,[51,52]

(Author list continued on next page)

Circulating levels of adiponectin, an adipocyte-secreted protein associated with cardiovascular and metabolic risk, are highly heritable. To gain insights into the biology that regulates adiponectin levels, we performed an exome array meta-analysis of 265,780 genetic variants in 67,739 individuals of European, Hispanic, African American, and East Asian ancestry. We identified 20 loci associated with adiponectin, including 11 that had been reported previously ($p < 2 \times 10^{-7}$). Comparison of exome array variants to regional linkage disequilibrium (LD) patterns and prior genome-wide association study (GWAS) results detected candidate variants ($r^2 > .60$) spanning as much as 900 kb. To identify potential genes and mechanisms through which the previously unreported association signals act to affect adiponectin levels, we assessed cross-trait associations, expression quantitative trait loci in subcutaneous adipose, and biological pathways of nearby genes. Eight of the nine loci were also associated ($p < 1 \times 10^{-4}$) with at least one obesity or lipid trait. Candidate genes include *PRKAR2A*, *PTH1R*, and *HDAC9*, which have been suggested to play roles in adipocyte differentiation or bone marrow adipose tissue. Taken together, these findings provide further insights into the processes that influence circulating adiponectin levels.

Introduction

Adiponectin is an adipose tissue-derived hormone that affects energy homeostasis and may link adiposity with the risk of type 2 diabetes (T2D), hyperinsulinemia, and metabolic syndrome.[1,2] Higher serum concentrations of adiponectin are associated with protection against inflammation and lower risk for obesity, cardiovascular disease, and T2D.[1,3,4] Genetic overlap has been observed between adiponectin levels and metabolic syndrome, as well as the metabolic syndrome-related traits of high-density lipoprotein (HDL) cholesterol and plasma insulin.[5,6]

[1]Department of Genetics, University of North Carolina at Chapel Hill, Chapel Hill, NC 27599, USA; [2]The Wellcome Trust Centre for Human Genetics, University of Oxford, Oxford OX3 7FZ, UK; [3]Department of Biological Sciences, Faculty of Arts and Sciences, Eastern Mediterranean University, Famagusta, Cyprus; [4]Novo Nordisk Foundation Center for Protein Research, Faculty of Health and Medical Sciences, University of Copenhagen, Copenhagen 2200, Denmark; [5]DTU Health Technology, Technical University of Denmark, Lyngby 2800, Denmark; [6]Genetics of Complex Traits, University of Exeter Medical School, Royal Devon & Exeter Hospital, Exeter EX2 5DW, UK; [7]Research Centre for Optimal Health, School of Life Sciences, University of Westminster, London, UK; [8]The Charles Bronfman Institute for Personalized Medicine, Icahn School of Medicine at Mount Sinai, New York, NY 10029, USA; [9]Department of Genetics, Harvard Medical School, Boston, MA 02115, USA; [10]Division of Endocrinology and Center for Basic and Translational Obesity Research, Boston Children's Hospital, Boston, MA 02115, USA; [11]Broad Institute of MIT and Harvard, Cambridge, MA 02142, USA; [12]University Center for Primary Care and Public Health, University of Lausanne, Lausanne 1010, Switzerland; [13]Swiss Institute of Bioinformatics, Lausanne 1015, Switzerland; [14]Division of Epidemiology, Department of Medicine, Vanderbilt-Ingram Cancer Center, Vanderbilt Epidemiology Center, Vanderbilt University School of Medicine, Nashville, TN 37203-1738, USA; [15]Genetics of Obesity and Related Metabolic Traits Program, Icahn School of Medicine at Mount Sinai, New York, NY 10029, USA; [16]MRC Epidemiology Unit, University of Cambridge, Cambridge CB2 0QQ, UK; [17]Carolina Population Center, University of North Carolina at Chapel Hill, Chapel Hill, NC 27516, USA; [18]Department of Family Medicine and Public Health, University of California, San Diego, CA 92093, USA; [19]Department of Epidemiology, Erasmus University Medical Center, Rotterdam 3015CN, the Netherlands; [20]Joseph J. Zilber School of Public Health, University of Wisconsin-Milwaukee, Milwaukee, WI 53201, USA; [21]Cardiovascular Health Research Unit, Department of Medicine, University of Washington, Seattle, WA 98101, USA; [22]Department of Biostatistics, University of Washington, Seattle, WA 98101, USA; [23]Medical Department III – Endocrinology, Nephrology, Rheumatology, University of Leipzig, Leipzig 4103, Germany; [24]Department of Biostatistics and Center for Statistical Genetics, University of Michigan, Ann Arbor, MI 48109, USA; [25]Office of Population Studies Foundation, Inc, Cebu City, Philippines; [26]Department of Nutrition and Dietetics, University of San Carlos, Cebu City, Philippines; [27]Novo Nordisk Foundation Center for Basic Metabolic Research, Faculty of Health and Medical Sciences, University of Copenhagen, Copenhagen 2200, Denmark; [28]Department of Internal Medicine, Erasmus MC University Medical Center Rotterdam, Rotterdam 3000 CA, the Netherlands; [29]Division of Preventive Medicine, Brigham and Women's Hospital, Boston, MA 02215, USA; [30]Harvard Medical School, Boston, MA 02115, USA; [31]The Institute for Translational Genomics and Population Sciences, Department of Pediatrics, LABioMed at Harbor-UCLA Medical Center, Torrance, CA 90502, USA; [32]Department of Twin Research and Genetic Epidemiology, Kings College London, London SE1 7EH, UK; [33]Division of Statistical Genomics, Department of Genetics, Washington University School of Medicine, St. Louis, MO 63110, USA; [34]National Heart, Lung, and Blood

(Affiliations continued on next page)

Peter Kovacs,[23] Jennifer Kriebel,[37,38] Markku Laakso,[53] Leslie A. Lange,[54] Terho Lehtimäki,[55,56] Jin Li,[43] Ruifang Li-Gao,[57] Lars Lind,[58] Jian'an Luan,[16] Leo-Pekka Lyytikäinen,[59,60] Stuart MacGregor,[61] David A. Mackey,[62,63] Anubha Mahajan,[2,64] Massimo Mangino,[32,65] Satu Männistö,[48] Mark I. McCarthy,[2,64,66] Barbara McKnight,[22] Carolina Medina-Gomez,[28,42] James B. Meigs,[67,68,69] Sophie Molnos,[37,38] Dennis Mook-Kanamori,[57,70] Andrew P. Morris,[2,71] Renee de Mutsert,[57] Mike A. Nalls,[72,73] Ivana Nedeljkovic,[19] Kari E. North,[35] Craig E. Pennell,[74] Aruna D. Pradhan,[29,30] Michael A. Province,[33] Olli T. Raitakari,[75,76,77] Chelsea K. Raulerson,[1] Alex P. Reiner,[39] Paul M. Ridker,[29,30] Samuli Ripatti,[11,78,79] Neil Roberston,[2,64] Jerome I. Rotter,[31] Veikko Salomaa,[48] America A. Sandoval-Zárate,[79] Colleen M. Sitlani,[21] Tim D. Spector,[32] Konstantin Strauch,[80,81] Michael Stumvoll,[23] Kent D. Taylor,[31] Betina Thuesen,[82] Anke Tönjes,[23] Andre G. Uitterlinden,[28,42] Cristina Venturini,[32] Mark Walker,[83] Carol A. Wang,[74] Shuai Wang,[41] Nicholas J. Wareham,[16] Sara M. Willems,[16] Ko Willems van Dijk,[84,85,86] James G. Wilson,[87] Ying Wu,[1] Jie Yao,[31] Kristin L. Young,[35] Claudia Langenberg,[16] Timothy M. Frayling,[6] Tuomas O. Kilpeläinen,[27,88] Cecilia M. Lindgren,[2,11,89,92] Ruth J.F. Loos,[8,90,92,*] and Karen L. Mohlke[1,92,*]

Mendelian randomization (MR) studies have suggested a causal role for adiponectin in metabolic syndrome and insulin sensitivity, but not coronary artery disease, insulin resistance, or T2D.[7–10] Experimental manipulations in mice have demonstrated that acute depletion of adiponectin results in systemic insulin resistance and poor lipid homeostasis, leading to hyperlipidemia.[11–13] Thus, understanding the pathophysiology of adiponectin levels may lead to therapeutic targets for the prevention and treatment of cardiovascular disease.[2,14,15]

Circulating levels of adiponectin are under substantial genetic influence. Twin and family studies have estimated that 30%–70% of the variability in adiponectin levels can be explained by genetic variation.[16–18] The largest

Institute, Bethesda, MD 20892, USA; [35]Department of Epidemiology, Gillings School of Global Public Health, University of North Carolina at Chapel Hill, Chapel Hill, NC 27599, USA; [36]Carolina Center for Genome Sciences, Chapel Hill, NC 27599, USA; [37]Research Unit of Molecular Epidemiology, Institute of Epidemiology, Helmholtz Zentrum München Research Center for Environmental Health, München-Neuherberg 85764, Germany; [38]German Center for Diabetes Research, München-Neuherberg 85765, Germany; [39]Public Health Sciences Division, Fred Hutchinson Cancer Research Center, Seattle, WA 98109, USA; [40]Laboratory of Epidemiology and Population Sciences, National Institute on Aging, NIH, Bethesda, MD 20892, USA; [41]Department of Biostatistics, Boston University School of Public Health, Boston, MA 2118, USA; [42]Department of Epidemiology, Erasmus MC University Medical Center Rotterdam, Rotterdam 3000 CA, the Netherlands; [43]Department of Medicine, Division of Cardiovascular Medicine, Stanford University, Palo Alto, CA 94304, USA; [44]Stanford Cardiovascular Institute, Stanford University of Medicine, Palo Alto, CA 94304, USA; [45]Department of Medical Sciences, Molecular Epidemiology and Science for Life Laboratory, Uppsala University, Uppsala 75185, Sweden; [46]Stanford Diabetes Research Center, Stanford University, Stanford, CA 94305, USA; [47]Division of Endocrinology, Diabetes, and Metabolism, Ohio State University, Columbus, OH 43210, USA; [48]Department of Public Health Solutions, National Institute for Health and Welfare, Helsinki 00271, Finland; [49]Department of Clinical Physiology, Tampere University Hospital, Tampere 33522, Finland; [50]Department of Clinical Physiology, Finnish Cardiovascular Research Center - Tampere, Faculty of Medicine and Health Technology, Tampere University, Tampere 33522, Finland; [51]Department of Medicine, Albert Einstein College of Medicine, Bronx, NY 10461, USA; [52]Department of Epidemiology and Population Health, Albert Einstein College of Medicine, Bronx, NY 10461, USA; [53]Institute of Clinical Medicine, Internal Medicine, University of Eastern Finland and Kuopio University of Hospital, Kuopio 70029 KYS, Finland; [54]Division of Biomedical Informatics and Personalized Medicine, Department of Medicine, University of Colorado-Denver, Denver, CO 80045, USA; [55]Department of Clinical Chemistry, Fimlab Laboratories, Tampere 33520, Finland; [56]Department of Clinical Chemistry, Finnish Cardiovascular Research Center - Tampere, Faculty of Medicine and Health Technology, Tampere University, Tampere 33522, Finland; [57]Department of Clinical Epidemiology, Leiden University Medical Center, Leiden 2333 ZA, the Netherlands; [58]Department of Medical Sciences, Uppsala University, Uppsala 75185, Sweden; [59]Department of Clinical Chemistry, Fimlab Laboratories, Tampere 33522, Finland; [60]Department of Clinical Chemistry, Finnish Cardiovascular Research Center - Tampere, Faculty of Medicine and Health Technology, Tampere University, Tampere 33521, Finland; [61]QIMR Berghofer Medical Research Institute, Brisbane, QLD 4006, Australia; [62]Faculty of Health and Medical Sciences, The University of Western Australia, Perth, WA 6009, Australia; [63]Centre for Ophthalmology and Visual Science, Lions Eye Institute, The University of Western Australia, Perth, WA 6009, Australia; [64]Oxford Centre for Diabetes, Endocrinology and Metabolism, Radcliffe Department of Medicine, University of Oxford, Oxford OX3 7FZ, UK; [65]NIHR Biomedical Research Centre, Guy's and St Thomas' Foundation Trust, London SE1 9RT, UK; [66]Oxford NIHR Biomedical Research Centre, Oxford University Hospitals Trust, Oxford OX3 7FZ, UK; [67]Division of General Internal Medicine, Massachusetts General Hospital, Boston, MA 02114, USA; [68]Department of Medicine, Harvard Medical School, Boston, MA 02115, USA; [69]Program in Population and Medical Genetics, Broad Institute, Cambridge, MA 02114, USA; [70]Department of Public Health and Primary Care, Leiden University Medical Center, Leiden 2334 ZA, the Netherlands; [71]Department of Biostatistics, University of Liverpool, Liverpool L69 3GL, UK; [72]Laboratory of Neurogenetics, National Institute on Aging, NIH, Bethesda, MD 20892, USA; [73]Data Tecnica International, Glen Echo, MD 20812, USA; [74]School of Medicine and Public Health, Faculty of Medicine and Health, The University of Newcastle, Newcastle, NSW 2305, Australia; [75]Centre for Population Health Research, University of Turku and Turku University Hospital, Turku, Finland; [76]Research Centre of Applied and Preventive Cardiovascular Medicine, University of Turku, Turku, Finland; [77]Department of Clinical Physiology and Nuclear Medicine, Turku University Hospital, Turku, Finland; [78]Public Health, University of Helsinki, Helsinki 00014, Finland; [79]Institute for Molecular Medicine Finland, Helsinki 00014, Finland; [80]Institute of Genetic Epidemiology, Helmholtz Zentrum München - German Research Center for Environmental Health, Neuherberg 85764, Germany; [81]Chair of Genetic Epidemiology, Institute of Medical Informatics, Biometry and Epidemiology, Ludwig-Maximilians-Universität, Munich 81377, Germany; [82]Center for Clinical Research and Disease Prevention, Bispebjerg and Frederiksberg Hospital, The Capital Region, Copenhagen 2400, Denmark; [83]Institute of Cellular Medicine, The Medical School, Newcastle University, Newcastle, UK; [84]Department of Internal Medicine, Division of Endocrinology, Leiden University Medical Center, Leiden 2333 ZA, the Netherlands; [85]Einthoven Laboratory for Experimental Vascular Medicine, Leiden 2333 ZA, the Netherlands; [86]Department of Human Genetics, Leiden University Medical Center, Leiden 2333 ZA, the Netherlands; [87]Department of Physiology and Biophysics, University of Mississippi Medical Center, Jackson, MS 39216, USA; [88]Department of Environmental Medicine and Public Health, Icahn School of Medicine at Mount Sinai, New York, NY 10029, USA; [89]Big Data Institute, Nuffield Department of Medicine, University of Oxford, Oxford OX3 7LF, UK; [90]The Mindich Child Health and Development Institute, Ichan School of Medicine at Mount Sinai, New York, NY 10029, USA
[91]These authors contributed equally to this work
[92]These authors contributed equally to this work
*Correspondence: ruth.loos@mssm.edu (R.J.F.L.), mohlke@med.unc.edu (K.L.M.)
https://doi.org/10.1016/j.ajhg.2019.05.002.

adiponectin genome-wide association study (GWAS) meta-analysis performed to date tested associations between ~2.4 million variants, imputed to the HapMap reference panel, in up to 35,355 individuals primarily of European ancestry (83%) and identified 12 loci, including *ADIPOQ* (MIM: 605441), which encodes the adiponectin protein, and *CDH13* (MIM: 601364), which encodes cadherin-13, a receptor that binds to circulating adiponectin.[14] A subsequent adiponectin GWAS meta-analysis in up to 18,079 East Asians, using HapMap-imputed variants, identified one additional locus near *WDR11-FGFR2* (MIM: 606417, 176943).[19] These common genetic variants accounted for only 5% of the variance in adiponectin levels.[14,19,20] Further investigation into the genetic basis for adiponectin levels and the associated loci would provide further insight into the genetic architecture and biological processes influencing adiponectin.

To discover and characterize candidate loci influencing circulating levels of adiponectin in order to further understand its role in insulin sensitivity and related traits, we combined exome array association results of up to 67,739 individuals from four ancestries (60,465 European, 3,271 African, 2,568 East Asian, and 1,435 Hispanics) to conduct the largest genetic analysis of adiponectin levels to date. Exome-based association studies, containing mostly nonsynonymous variants (n = 213,082, 80.2% of all variants in the analysis), may potentially provide results with more direct biological interpretability. However, nonsynonymous variant associations do not constitute sufficient evidence to implicate the target gene(s) underlying an association signal.[21] Therefore, we used extent of linkage disequilibrium (LD), gene expression-variant association data, and pathway analyses to suggest genes and mechanisms through which the previously unreported variants may act to affect adiponectin levels.

Material and Methods

Study Design and Participants

Our meta-analysis consisted of 25 studies (28 datasets) comprising up to 67,739 adult individuals (≥18 years) of the following ancestries: (1) European (n ≤ 60,465), (2) East Asian (n ≤ 2,568), (3) African American (n ≤ 3,271), and (4) Hispanic (n ≤ 1,435). All participating institutions and coordinating centers approved this project, and informed consent was obtained from all study participants. In our primary discovery analyses, we combined data of all ancestries for both sex-specific and sex-combined analyses (Figure S1). Study-specific design, sample quality control, and descriptive statistics are provided in Tables S1–S3.

Genotype Calling

Each of the 25 contributing studies followed a standardized protocol and performed genotype calling of variants on the Illumina HumanExome Beadchip using the designated manufacturer's software. Study-specific quality control measures of the genotyped variants were implemented before association analyses (Table S2). We excluded variants with a call rate < 98%, Hardy Weinberg equilibrium $p < 1 \times 10^{-6}$, or large allele frequency deviations from the reference populations (>0.60 for all ancestry analyses and >0.30 for ancestry-specific population analyses).

Statistical Analyses

We created residuals of adiponectin levels (in μg/mL) after adjustment for age, body mass index (BMI), and principal components (PCs, derived from GWAS data, variants with minor allele frequency [MAF] > 1% on the exome array, or ancestry-informative markers on the exome array), as well as any study-specific covariates, using a linear regression model. For studies with unrelated individuals, residuals were calculated separately by sex; for family-based studies, sex was included as a covariate in the model. Additionally, residuals for case-control studies were calculated in case subjects and control subjects separately. Finally, residuals were subjected to inverse normal transformation to obtain distributions with a mean of 0 and a standard deviation of 1, yielding approximately normally distributed trait values for downstream analyses. In additional analyses performed without adjustment for BMI and adjusted for fat percentage instead of BMI, results were similar (Figures S2–S5, Table S4) with one additional locus detected in models unadjusted for BMI (rs900399 in *LEKR1* [MIM: 613536]); other signals became less significant.

Each study performed single-variant association analyses between inverse normal-transformed adiponectin levels (adjusted for age, sex, BMI, and other study-specific covariates) and exome array variants, including up to 28,868 common (MAF ≥ 5%) and 236,912 low-frequency (1% ≤ MAF < 5%) or rare (MAF < 1%) variants, using either RAREMETALWORKER or RVTEST (Table S2).[22,23] All analyses were performed in sex-combined and sex-specific groups, accounting for potential cryptic relatedness (kinship matrix), in a linear mixed model.

We applied a centralized quality control procedure to individual cohort association summary statistics using EasyQC[24] to: (1) assess adiponectin transformation, (2) compare allele frequency alignment to the 1000 Genomes Project phase 1 reference panel to detect strand errors, and (3) examine quantile-quantile plots per study to detect population stratification, cryptic relatedness, and genotype biases.

Summary statistics were meta-analyzed using fixed-effects inverse-variance analyses in an all-ancestry, sex-combined, additive model, and variant associations that reached $p < 2 \times 10^{-7}$ were considered array-wide significant (Bonferroni corrected for multiple testing; 0.05/265,780 variants).[21,25,26] Meta-analyses were carried out using RAREMETAL[27] by two analysts at two sites in parallel. For all significant variants identified in the meta-analyses, we tested for differences between women-specific and men-specific beta estimates using EasyStrata.[28] Each variant that reached $p_{sexhet} < 0.05/(\text{number of variants tested})$ was considered significant. In secondary analyses, we also performed analyses with adiponectin levels unadjusted for BMI and with adiponectin levels adjusted for fat percentage instead of BMI, as well as analyses stratified by sex (Figures S2–S8).

For gene-based analyses, we applied the sequence kernel association test (SKAT)[29] and variable threshold (VT)[30] gene-based methods in RAREMETAL using two different sets of criteria (broad and strict).[26,31] These two sets of criteria were used to select variants with a MAF < 5% within each ancestry group based on coding variant annotation from five prediction algorithms (PolyPhen2, HumDiv and HumVar, LRT, MutationTaster, and SIFT). The broad gene-based tests comprised of nonsense, stop-loss, splice site, and missense variants annotated as damaging by at least one algorithm

mentioned above. The strict gene-based tests included only nonsense, stop-loss, splice site, and missense variants annotated as damaging by all five algorithms. Statistical significance for gene-based tests was set at a Bonferroni-corrected threshold of $p < 2.5 \times 10^{-6}$ based on approximately 20,000 genes.[32] As secondary analyses were nested and/or highly correlated with the primary analysis, we chose the same stringent Bonferroni-corrected significance threshold for all analyses.

We also used the RAREMETAL R package to identify independent association signals across all ancestries and European (sex-combined and sex-specific) meta-analysis results. In 1 Mb windows centered on each lead (most significantly associated) variant, we performed sequential rounds conditioning on the lead variant to identify additional signals at $p < 2 \times 10^{-7}$.

Assessment for Bias

To address possible collider bias[33,34] in our significant association results, we used the summary statistics from an exome-chip study of BMI, a GWAS of body fat percentage, and our adiponectin results from models unadjusted for BMI or fat percentage.[26] Our principal aim was to exclude the possibility that some of the discovered adiponectin-SNP associations are entirely driven by the association of the SNPs and obesity traits correlated with adiponectin levels. To this end, BMI and fat percentage-adjusted associations were corrected for potential bias due to phenotypic correlation between adiponectin levels and each covariate as well as possible association between each variant and covariate. Strength and significance of association with adiponectin unadjusted, adjusted for BMI, or adjusted for fat percentage were compared with each other, and those of covariates and corrected statistics. Corrected effect sizes were estimated using the following equation:[33]

$$\beta_{\text{corrected}} = \beta_{\text{adiponectin adj. covariate}} + \left(\beta_{\text{covariate}} \times \rho_{\text{covariate x adiponectin}}\right)$$

where $\rho_{\text{BMI x adiponectin}} = -0.31$ and $\rho_{\text{fat percent x adiponectin}} = -0.27$.[35]

Associations with Cardiometabolic Traits

We evaluated each of the nine previously unreported loci that we detect here for association in prior adiponectin GWAS meta-analyses from ADIPOGen[14] and AGEN[19] and with other cardiometabolic traits and diseases. For these traits, we examined existing genome- and exome-wide meta-analysis results from consortia including GIANT (BMI[26] and waist-to-hip-ratio adjusted for BMI[36]), GLGC (total cholesterol, HDL, LDL, and triglycerides),[25] T2D,[21] and MAGIC (HbA1c, fasting insulin, fasting glucose, 2-hour glucose).[37–40] We also examined the UK Biobank for associations with cardiometabolic traits and diseases. In addition, PhenoScanner was used to perform a PheWAS on all available traits, plasma proteins, and metabolites. We report proteins and metabolites when the lead exome variant and the variant most strongly associated with the protein or metabolite within 1 Mb exhibit high pairwise LD ($r^2 > 0.80$). We did not identify any plasma proteins that met our criteria.

Annotation and Colocalization of Association Signals with eQTL Data

We examined whether any of the lead exome-wide associated variants were associated with expression (FDR < 1% for METSIM for rigor; FDR < 5% for GTEx as available) of nearby transcripts located within 1 Mb in subcutaneous or visceral adipose tissue (eQTLs).[41,42] Briefly, gene expression was measured in subcutaneous adipose tissue in 770 Finnish male participants from the Metabolic Syndrome in Men Study (METSIM) using the Affymetrix U219 microarray. From GTEx v7, we used gene expression data from 385 subcutaneous and 315 visceral adipose samples. Variant-trait and eQTL signals may colocalize when the lead exome variant and the variant most strongly associated with the expression level of the corresponding transcript (eSNP) exhibit high pairwise LD ($r^2 > 0.80$). For such signals identified in the METSIM eQTL data, we also further assessed colocalization using reciprocal conditional analyses to test the association between the lead exome variant and transcript level when the eSNP was also included in the model, and vice versa; we reported exome-wide and eQTL signals as colocalized if the association for the eSNP was not significant (FDR > 1%) when conditioned on the adiponectin-associated exome variant.

Gene Set Enrichment Analysis

We performed a gene set enrichment analysis based on the European summary statistics of variants from the adiponectin adjusted for BMI association results using EC-DEPICT. EC-DEPICT, designed for use in exome array analyses,[26,43] assesses enrichment for a group of 14,462 gene sets (including canonical pathways, protein-protein interaction networks, and mouse phenotypes) that have been "reconstituted" using large-scale co-expression data. Briefly, enrichment p values were calculated using 2,000 permutations of 378,141 European samples from the UK Biobank, where only variants present on both the ExomeChip and UK Biobank arrays were included for analysis.[26,44] The input data included genes directly containing the most significant nonsynonymous coding variant per locus, where loci were defined as ±1 Mb from the index variant. We performed EC-DEPICT analyses using variants with an association of $p < 5 \times 10^{-4}$ across (1) all variants and (2) variants with MAF < 5%. We considered a false discovery rate of less than 0.05 to be statistically significant.

We also performed a pathway analysis by applying PASCAL to the European exome-wide summary statistics from the adiponectin (adjusted for BMI) association results.[45] The method derives gene-based scores and subsequently tests for over-representation of high gene scores in pre-defined biological pathways. For the gene-based scores we performed both MAX and SUM estimations: the former being more powerful when the association is driven by a single variant in/near the focal gene, while the latter is preferred in case of allelic heterogeneity. We used both standard pathway libraries and dichotomized (Z-score > 3) reconstituted gene sets from DEPICT. A reference dataset from UK10K (TwinsUK[46] and ALSPAC[47] studies, n = 3,781) was used for LD estimation. Unlike EC-DEPICT, p value thresholds were not used to select input variants from the exome-wide data. Variants with MAF < 1% in the reference dataset were included in the analysis. To separate the contribution of coding (nonsynonymous and synonymous) variants, we performed PASCAL analyses across (1) all variants and (2) only coding variants. $p < 5 \times 10^{-5}$ was considered statistically significant after Bonferroni correction for multiple testing with 1,000 independent pathways.

Results

We conducted meta-analyses of single-variant association summary statistics, including data from up to 67,739 individuals from 25 studies (Tables S1–S3) across four ethnic

groups; 89% of individuals had European ancestry. Each study performed single-variant association analyses adiponectin adjusted for age, sex, and BMI and exome array variants, and summary statistics from each dataset were meta-analyzed using fixed-effects analyses in an all-ancestry, sex-combined, additive model.[21,25,26] In secondary analyses, we also examined adiponectin levels unadjusted for BMI, adiponectin levels adjusted for fat percentage instead of BMI, and models stratified by sex (Figures S2–S8). Participants were broadly representative of adults (age 18–95 years) of both sexes (51.2% male) with a wide distribution of BMI and adiponectin levels (Table S3).

Association Results

The primary sex-combined analysis of adiponectin levels adjusted for BMI identified variants ($p < 2.0 \times 10^{-7}$) at 11 known loci (in/near *LYPLAL1* [MIM: 616548], *IRS1* [MIM: 147545], *STAB1* [MIM: 608560], *ADIPOQ, ARL15* [MIM: unknown]*/FST* [MIM: 136470], *PDE3A* [MIM: 123805], *CLIP1* [MIM: 179838], *DNAH10* [MIM: 605884], *CMIP* [MIM: 610112], *CDH13*, and *PEPD* [MIM: 613230]) and 8 loci (in/near *KIF9* [MIM: 607910], *DALRD3* [MIM: unknown], *FAM13A* [MIM: 613299], *SLC39A8* [MIM: 608732], *SNX13* [MIM: 606589], *GIMAP7* [MIM: 616961], *RIC8B* [MIM: 609147], and *SLC38A8* [MIM: 615585]) (Tables 1 and S5; Figures 1, 2, S7, and S9). Lead variants at each locus were primarily common (MAF ≥ 5%), with the exception of one low-frequency variant at *SLC39A8* (rs13107325; MAF = 4.7%) and one rare variant at *SLC38A8* (rs145119400; MAF = 0.5%). An all-ancestry, women-only analysis identified an additional locus (rs1199354, *OPLAH* [MIM: 614243], MAF = 10.1%) that also exhibited significant sex heterogeneity ($p = 2.5 \times 10^{-5}$; Table 1; Figure S10). Low to moderate levels of heterogeneity were detected among the lead variants at each locus (Table S5). We further tested the association of adiponectin levels with aggregated variants within each gene by performing gene-based association tests; however, no additional loci were detected (Table S6).

To investigate the potential for collider bias in the adiponectin analysis resulting from adjusting for a correlated covariate, BMI, we investigated the behavior of variants associated with adiponectin adjusted for BMI in analyses of adiponectin without adjustment for BMI and analyses of BMI alone, estimating the effect of bias. Nearly all of the adiponectin-associated variants identified showed a genuine effect on adiponectin levels, and any bias caused by adjusting for BMI was minimal. Only one locus (*SLC39A8*; rs13107325) exhibited potential pleiotropy and/or a collider bias effect due to BMI adjustment (Table S7). It is possible that applying rank-based inverse normal transformation to the residuals as opposed to the adiponectin values could have reintroduced inflation from the covariates and identified false positive results.[48] However, examination of cohort-specific QQ plots, comparison of models unadjusted and adjusted for BMI, and the results from the collider bias analysis suggest any inflation is unlikely.

To identify additional association signals at the 20 significant loci, we implemented conditional analyses and identified 3 additional, already established loci that harbored multiple distinct variants associated with adiponectin: *ADIPOQ* (9 signals; $r^2 = 0.00–0.19$), *DNAH10-CCDC92* (2 signals; $r^2 = 0.07$; MIM: 614848), and *SLC38A8* (2 signals; $r^2 = 0.00$) (Table S8; Figure S11). These results are consistent with previous reports of multiple signals at these loci for adiponectin and/or other cardiometabolic traits.[49,50] While the exome array-based analysis does not fully characterize the number or identity of the signals due to the relatively low density of analyzed variants, these findings support the presence of multiple adiponectin association signals at these loci.

Other Trait Associations

To further characterize the lead variants, we examined their associations with a range of cardiometabolic traits, including anthropometric, blood pressure, glycemic, and lipid traits and T2D (Tables 2, S9, and S10). Of the nine loci, six have previously shown a genome-wide significant association ($p < 5 \times 10^{-8}$) with at least one additional cardiometabolic trait: WHRadjBMI (four loci), HDL cholesterol (three loci), fat free mass index (two loci), body fat percentage (two loci), hip circumference (two loci), diastolic blood pressure (two loci), systolic blood pressure (one locus), hypertension (one locus), and BMI (one locus). The adiponectin signal associated with the largest number of other traits is *SLC39A8*, which also exhibited suggestive pleiotropy in the collider bias analysis (Table S7). That lead variant (p.Ala391Thr; rs13107325) has previously been shown to associate with BMI, blood pressure traits, HDL, other obesity-related traits, as well as Crohn disease and schizophrenia.[51] An additional PheWAS was performed in all available traits, plasma proteins, and metabolites (Tables S11 and S12). The additional trait associations may suggest pleiotropic or mediating effects at these loci.

Extent of LD Surrounding Exome Array Signals

The identification of nonsynonymous variant associations has the potential to pinpoint functional genes. However, evidence of association is not sufficient to conclude that these variants or genes have causal effects on trait levels. To assess the potential role of variants at previously unreported adiponectin loci, we assessed the LD with neighboring variants using 1000 Genomes Phase 3 for the European population to estimate the extent of the locus and to identify additional candidate variants ($r^2 > 0.80$) (Figures 1, 2, and S9; Table 2). Variants at four loci (nearest genes *KIF9*, *DALRD3*, *GIMAP7*, and *OPLAH*) are each part of wider LD blocks containing between 37 and 330 variants that span a distance of 35 to 819 kb including multiple genes; three of these loci include nonsynonymous variants in more than one gene (Figures 1 and 2; Table 2). For example, at the *KIF9* locus (Figure 1, Table 2),

Table 1. Adiponectin Loci in Sex-Combined and Sex-Specific Meta-analyses (Additive, adjBMI)

							Sex-Combined			Women			Men			Sex Diff.
Variant	**Chr**	**Position**	**Nearest Gene**	**Annotation**	**EA**	**EAF**	**Effect**	**p**	**n**	**Effect**	**p**	**n**	**Effect**	**p**	**n**	**p[a]**
Loci Achieving Exome-wide Significance																
rs2276853	3	47,282,303	*KIF9*	missense (p.Arg638Gly)	A	0.594	−0.033	3.35E−08	65,521	−0.039	1.98E−06	31,788	−0.029	4.18E−04	33,733	4.17E−01
rs3087866	3	49,054,692	*DALRD3*	missense (p.Gln299Arg)	C	0.786	−0.040	2.14E−08	65,521	−0.034	5.88E−04	31,788	−0.046	3.67E−06	33,733	3.86E−01
rs13133548	4	89,740,128	*FAM13A*	intronic	A	0.489	−0.039	5.91E−12	65,521	−0.033	3.24E−05	31,788	−0.041	1.98E−07	33,733	4.61E−01
rs13107325	4	103,188,709	*SLC39A8*	missense (p.Ala391Thr)	T	0.047	0.072	1.05E−07	59,606	0.078	1.13E−05	31,788	0.050	1.25E−02	33,733	2.98E−01
rs10282707	7	17,911,038	*SNX13*	intronic	T	0.383	−0.040	1.96E−10	56,826	−0.024	1.07E−02	24,421	−0.053	3.44E−10	32,405	2.00E−02
rs3735080	7	150,217,309	*GIMAP7*	missense (p.Arg83Cys)	T	0.245	−0.049	7.70E−13	65,521	−0.036	2.72E−04	31,788	−0.057	6.22E−10	33,733	1.05E−01
rs11993554	8	145,111,529	*OPLAH*	synonymous (p.Phe612Phe)	G	0.101	0.030	3.75E−03	61,431	0.076	9.76E−08	29,427	−0.011	4.66E−01	32,004	2.52E−05
rs10861661	12	107,174,646	*RIC8B*	intronic	C	0.229	−0.040	1.75E−09	59,489	−0.035	4.74E−04	27,455	−0.046	3.17E−06	32,034	4.42E−01
rs145119400	16	84,075,593	*SLC38A8*	missense (p.Pro57Leu)	A	0.005	−0.300	8.95E−13	59,107	−0.306	1.78E−03	28,412	−0.296	1.80E−10	30,695	9.23E−01
Previously Reported Loci Achieving Exome-wide Significance																
rs2791552	1	219,652,033	*LYPLAL1*	intergenic	C	0.676	0.676	1.75E−14	55,387	−0.055	8.97E−09	26,391	−0.054	7.16E−09	28,996	9.68E−01
rs2943641	2	227,093,745	*IRS1*	intergenic	C	0.646	0.646	1.76E−21	65,521	−0.048	2.21E−08	31,788	−0.069	2.56E−16	33,733	7.30E−02
rs13303	3	52,558,008	*STAB1*	missense (p.Met2506Thr)	C	0.569	0.569	2.69E−21	61,431	0.061	8.28E−13	29,427	0.060	4.74E−12	32,004	9.53E−01
rs17366568	3	186,570,453	*ADIPOQ*	ncRNA/exonic	A	0.118	0.118	1.43E−145	51,153	−0.216	1.61E−64	31,788	−0.239	5.86E−89	25,849	1.97E−01
rs4311394	5	53,300,662	*ARL15*	intronic	G	0.257	0.257	1.68E−10	59,931	−0.046	1.54E−06	28,914	−0.044	3.84E−06	31,017	9.13E−01
rs7134375	12	20,473,758	*PDE3A*	intergenic	A	0.410	0.410	3.69E−20	65,521	0.054	2.88E−11	31,788	0.053	5.36E−11	33,733	9.14E−01
rs11057405	12	122,781,897	*CLIP1*	intronic	A	0.086	0.086	2.90E−14	65,521	−0.092	1.74E−10	31,788	−0.068	1.24E−06	33,733	2.29E−01
rs11057353	12	124,265,687	*DNAH10*	missense (p.Ser167Pro)	C	0.645	0.645	2.74E−19	65,521	0.061	3.47E−13	31,788	0.047	2.19E−08	33,733	2.17E−01
rs2925979	16	81,534,790	*CMIP*	intronic	C	0.693	0.693	1.38E−37	61,801	0.093	6.72E−26	29,767	0.072	1.91E−16	32,034	8.80E−02
rs3865188	16	82,650,717	*CDH13*	intergenic	T	0.472	0.472	1.14E−08	59,420	−0.042	7.28E−07	28,616	−0.027	1.11E−03	30,804	2.27E−01
rs4805885	19	33,906,123	*PEPD*	intronic	C	0.603	0.603	2.85E−25	61,431	0.076	4.63E−19	29,427	0.052	5.77E−28	32,004	5.20E−02

Loci achieving exome-wide significance ($p < 2E{-}07$) in sex-combined and/or sex-specific all-ancestry meta-analyses. Beta effect size from an additive model corresponding to the effect allele for inverse-normal transformed adiponectin levels adjusted for age, BMI, and other study-specific covariates. The smallest p value for each variant is shown in bold. Physical positions based on hg19. Abbreviation: Chr, chromosome; EA, effect allele; EAF, effect allele frequency; n, sample size.

[a]Test for sex difference; values significant at the table-wide Bonferroni threshold of $0.05/20 = 2.5E{-}03$

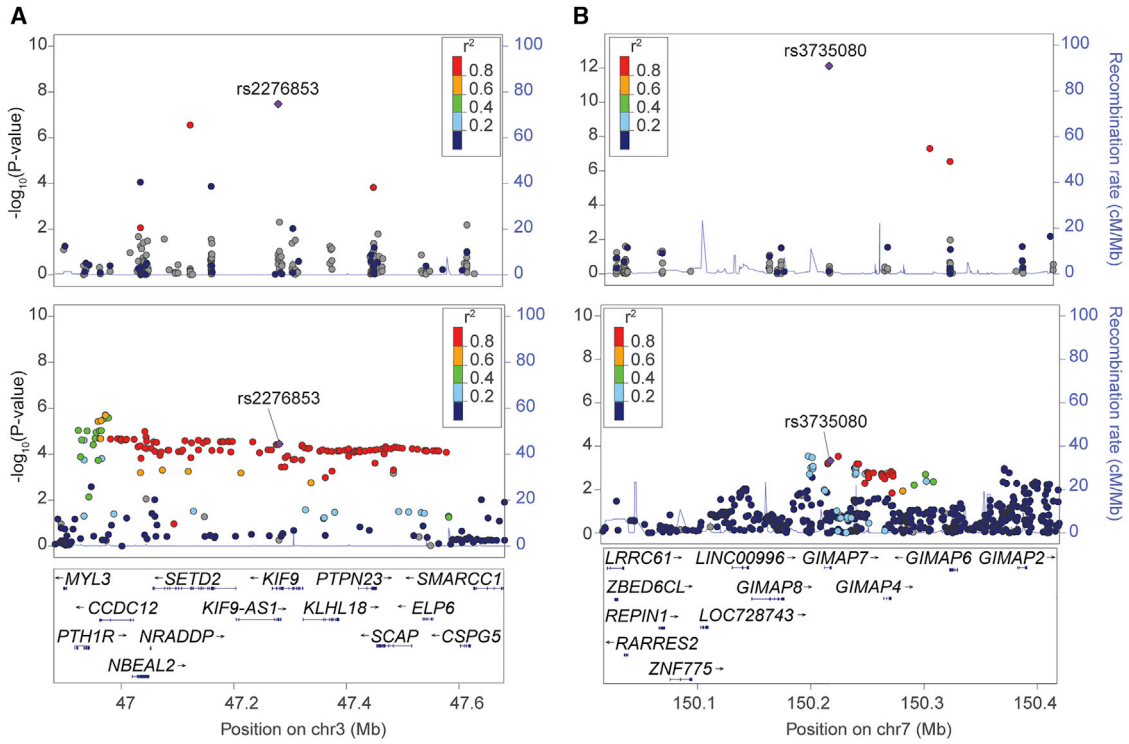

Figure 1. Loci in Adiponectin Exome-wide Meta-analysis Located within Broader Trait-Associated Regions
KIF9 locus (A) and *GIMAP7* locus (B). Each point represents a variant in the meta-analysis, plotted with hg19 genomic position on the x axis and p value (on a $-\log_{10}$ scale) on the y axis. The upper plots show the current exome-wide meta-analysis, and the lower plots show the genome-wide ADIPOGen consortium meta-analysis.[14] In each plot, the lead variant identified in the exome array meta-analysis is represented in purple, and the color of all other variants indicate the LD with the lead variant in European ancestry haplotypes from the 1000 Genomes Phase 3 reference panel. In both examples, the lead variant from the exome-wide analysis may not be the best representative of the adiponectin-associated signal.

the lead variant, rs2276853, encodes *KIF9* p.Arg638Gly. However, 330 additional variants spanning nearly 600 kb are in high LD with the lead variant ($r^2 > 0.80$), including nonsynonymous variants in four additional genes (*SETD2* [MIM: 612778], *SCAP* [MIM: 601510], *NBEAL2* [MIM: 614169], *PTPN23* [MIM: 606584]). The wide LD regions motivated further investigation of possible mechanisms and gene(s) through which candidate variant(s) act to affect adiponectin levels.

Most of the nonsynonymous variants identified in the meta-analysis have low or inconsistent evidence of functional consequences in algorithms, suggesting that other variants may have functional effects (Table S13). Because the exome array captures only a limited set of variants and the extent of LD surrounding each of locus can be vast, we further interrogated each locus to determine whether the lead variant is the best representative of the association signal. To do so, we examined the association results of the exome array loci within the ADIPOGen Consortium genome-wide meta-analysis of adiponectin levels (n = 35,355; HapMap imputed).[14] At six loci (*KIF9*, *GIMAP7*, *DALRD3*, *RIC8B*, *SNX13*, and *FAM13A*), a variant other than the exome array lead variant showed a more significant association with adiponectin (Figures 1 and 2, Table 2). For example, at the *KIF9* locus, genome-wide association results showed variants in moderate LD ($0.60 < r^2 <$ 0.80) with the lead exome array variant that had stronger association with adiponectin levels.[14] These variants are located near *PTH1R* (MIM: 168468), and reduced *PTH1R* leads to increased adipocyte differentiation and higher adiponectin levels (Table S14),[52] suggesting *PTH1R* as a strong candidate gene at this locus. A seventh locus, *SLC38A8*, could not be compared to the genome-wide association data because neither the lead variant nor either of the two variants in strong LD ($r^2 > 0.80$) with it were evaluated by ADIPOGen.[14] These genome-wide analyses suggest that the genes harboring the lead exome array variants may not be the best candidate genes and that the association signals may act via other variants and possibly other nearby genes instead.

Comparison with eQTL Signals

To aid in the identification of candidate genes at the nine previously unreported association signals, we examined whether any of the variants associated with adiponectin are colocalized (see Material and Methods) with expression levels of nearby transcripts in subcutaneous or visceral adipose tissue. For this analysis, we compared the pattern of variant association with adiponectin levels to the pattern of variant association in the expression quantitative trait locus (eQTL) analysis in GTEx[42] and the METSIM study (Table S15).[41] Two loci showed evidence

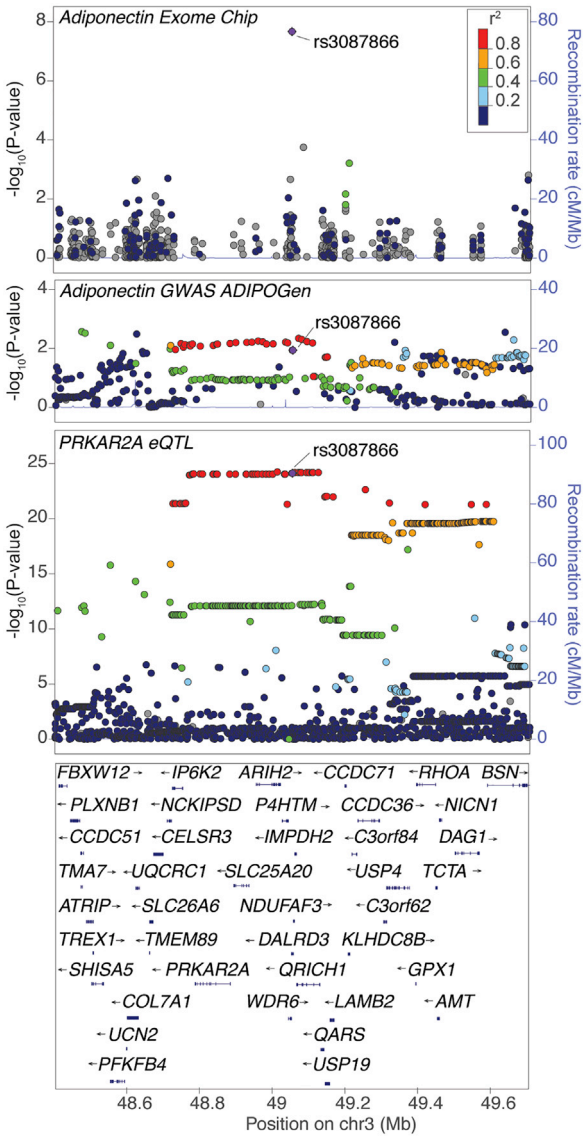

Figure 2. Subcutaneous Adipose eQTL for *PRKAR2A* Colocalizes with the *DALRD3* Adiponectin Exome-wide Locus
rs3087866 (purple diamond) shows the strongest association with adiponectin levels in the exome-wide meta-analysis (top plot). In the ADIPOGen genome-wide adiponectin meta-analysis (middle plot),[14] rs3087866 and 85 proxy variants ($r^2 > 0.80$; 1000Gp3) are nominally associated with adiponectin levels. The same variants exhibit the strongest association with expression of *PRKAR2A* in subcutaneous adipose tissue (lower plot).[41] Colocalized eQTL signals are also observed for *AMT* and *NICN1* (see Figure S12). Each point represents a variant, plotted with hg19 genomic position on the x axis and p value (on a $-\log_{10}$ scale) on the y axis. The color of all other variants indicates the LD with the lead variant in European ancestry haplotypes from the 1000 Genomes Phase 3 reference panel.

of colocalized associations. The adiponectin-associated variant rs13133548 is in high LD ($r^2 = 0.95$) with rs72614904, the variant most strongly associated with expression level of *FAM13A* ($\beta = 0.190$, $p = 8.10 \times 10^{-9}$); alleles associated with lower adiponectin are associated with higher *FAM13A* expression level. Consistent with these associations, *FAM13A* has been shown to control adipocyte lipolysis (Table S14).[53] The next adiponectin-associated variant rs3087866 is in high LD ($r^2 = 0.99$) with rs6446200, the variant most strongly associated with expression levels of *PRKAR2A* (MIM: 176910) ($\beta = 0.652$, $p = 5.79 \times 10^{-25}$; Figure 2), *AMT* ($r^2 = 0.92$, $\beta = -0.364$, $p = 1.14 \times 10^{-8}$), and *NICN1* (MIM: 611516) ($r^2 = 0.90$, $\beta = 0.408$, $p = 1.69 \times 10^{-11}$) (Figure S12). At this signal, alleles associated with lower adiponectin are associated with higher *PRKAR2A* and *NICN1* expression level, but lower *AMT* (MIM: 238310) expression level. The strongest eQTL association signal is with *PRKAR2A*, which encodes a subunit of cAMP-dependent protein kinase, an essential regulator of lipid and glucose metabolism that plays a role in energy homeostasis.[54] Although the exome array variants may not be the best representative variant for these association signals, the LD between the exome array variants and the lead eQTL variants is strong, suggesting that *FAM13A*, *PRKAR2A*, *AMT*, and *NICN1* are plausible candidate genes for regulatory effects at these loci.

Candidate Pathways

To further characterize the biological processes and candidate pathways enriched within the identified adiponectin-associated loci, we performed gene set enrichment analyses using PASCAL and EC-DEPICT.[26,43,45] The PASCAL analyses assuming single association signals from each locus (MAX score) showed significant ($p < 5 \times 10^{-5}$) evidence for enrichment in gene sets for the adipocyte differentiation-related ATXN1 protein-protein interaction sub-network[55] (Tables S16A, S16B, and S17), and the PASCAL analyses that considered multiple association signals from the same loci (SUM score) provided additional evidence for enrichment in gene sets for abnormal white adipose tissue physiology, decreased gonadal fat pad weight, and the adipogenesis-related NR3C1 protein-protein interaction sub-network (Tables S16C, S16D, and S17).[56] None of the gene sets from EC-DEPICT achieved statistical significance (FDR < 0.05), possibly due to sample size and the number of loci detected (especially for the analysis restricted to low-frequency and rare variants [MAF < 5%]) (Tables S18A and S18B). The enriched processes obtained with these approaches suggest that the adiponectin association signals may alter adipose tissue- and obesity-related pathways.

Discussion

This exome-array based meta-analysis of 265,780 variants in up to 67,739 individuals from four different ancestries identified 30 distinct signals in 20 loci associated with circulating adiponectin levels, including nine loci previously not reported to be associated with adiponectin. Two of the independent signals are located in regions that exhibit extensive LD, and comparison of lead exome array variants to the patterns of association in the previously performed, smaller ADIPOGen GWAS dataset[14] suggests the possible contribution of noncoding

Table 2. Biological Candidate Genes at Previously Unreported Adiponectin-Associated Loci

Lead Variant	EAF	Nearest Gene	n Variants $r^2 \geq 0.80$ (Distance kb)	n Variants $r^2 \geq 0.60$ (Distance kb)	Function/ Nonsynonymous Variants ($r^2 > 0.8$)	Adipose eQTL Gene ($p < 5 \times 10^{-8}$)	Other Trait Associations ($p < 1 \times 10^{-4}$)	Literature Candidate
rs2276853	0.59	*KIF9*	330 (597 kb)	353 (597 kb)	KIF9 (p.Arg638Gly)*; SETD2 (p.Pro1918His); *SCAP* (p.Val543Ile); *NBEAL2* (p.Arg511Gly); *PTPN23* (p.Ala818Thr)	–	WHRadjBMI, adiponectin, T2D	*PTH1R*
rs3087866	0.79	*DALRD3*	73 (819 kb)	210 (833 kb)	*DALRD3* (p.Gln299Arg)*	*AMT, NICN1, PRKAR2A, QRICH1*	FFMI, WHRadjBMI, Adiponectin, Menarche, T2D	*PRKAR2A*
rs13133548	0.49	*FAM13A*	41 (35 kb)	54 (35 kb)	–	*FAM13A*	BF%, HC, HDL, WHRadjBMI, Adiponectin, BMI, T2D, TG	*FAM13A*
rs13107325	0.05	*SLC39A8*	3 (51 kb)	4 (196 kb)	*SLC39A8* (p.Ala391Thr)*	–	BMI, BF%, DBP, FFMI, HC, HDL, HTN, SBP, WC, WHRadjBMI, Adiponectin, TG	*SLC39A8*
rs10282707	0.38	*SNX13*	9 (104 kb)	16 (130 kb)	–	–	HDL, TC	*HDAC9*
rs3735080	0.24	*GIMAP7*	278 (119 kb)	294 (146 kb)	*GIMAP7* (p.Arg83Cys)*; *GIMAP6* (p.Gly241Ser)	–	DBP, FFMI, HTN, SBP	*REPIN1; RARRES2*
rs11993554	0.10	*OPLAH*	37 (57 kb)	122 (107 kb)	*OPLAH* (p.Phe612Phe*, p.Arg31Gln, p.Val340Ile, p.Ser284Arg); *EPPK1* (p.Arg936Trp)	–	WHRadjBMI	*MAF1*
rs10861661	0.23	*RIC8B*	14 (134 kb)	16 (134 kb)	–	–	WHRadjBMI, HDL, TG, HC	*CRY1*
rs145119400	0.005	*SLC38A8*	2 (257 kb)	2 (257 kb)	*SLC38A8* (p.Pro57Leu)*	–	–	*CDH13; MBTPS1*

Biological candidate genes at each of the loci previously not shown to be association with adiponectin. Number of variants in moderate to strong linkage disequilibrium and the distance spanned obtained using data from 1000 Genomes Phase 3 and build hg19 (LDLink). Nonsynonymous variants noted with an asterisk (*) are the lead variants identified at each locus. eQTLs were identified in METSIM subcutaneous adipose and/or GTEx subcutaneous or visceral adipose tissues (see Table S15). Other trait associations were identified from available summary statistics from the ADIPOGen, DIAGRAM, GIANT, and GLGC consortia, along with the UK Biobank (see Tables S9–S11). Abbreviations: BMI, body mass index; BF%, body fat percentage; DBP, diastolic blood pressure; FFMI, fat free mass index; HC, hip circumference; HDL, high density lipoprotein cholesterol; HTN, hypertension; Menarche, age at menarche; SBP, systolic blood pressure; WC, waist circumference; WHRadjBMI, waist-hip-ratio adjusted for BMI.

variants acting on more distant candidate genes. eQTL colocalizations and evaluation of gene functions helped detect potential genes and mechanisms through which the variants may act to affect adiponectin levels. Candidate genes include *FAM13A*, *SLC39A8*, *PRKAR2A*, *PTH1R*, and *HDAC9*. Eight of the association signals have been found to be associated with other obesity and lipid traits; the evidence of association with adiponectin levels also guides interpretation of genes and mechanisms for these traits.

Once an association with a nonsynonymous variant is detected, it is simple to hypothesize a causal connection between the variant, the gene in which it is located, and the examined phenotype. We demonstrate that this assumption is often inaccurate, particularly with regards to common nonsynonymous variants identified through an exome array analysis. For example, the common (MAF = 0.41), adiponectin-associated variant, rs2276853, encodes missense variant p.Arg638Gly in *KIF9*, kinesin family member 9, a regulator of spindle dynamics localized to the nuclear envelope that is essential for mitosis.[57] Examination of the surrounding wide LD region using GWAS data from the previous ADIPOGen study[14] showed that moderately correlated variants 300 kb upstream near *PTH1R*, parathyroid hormone receptor 1, exhibited a more significant association with adiponectin levels. Reduced levels of *PTH1R* lead to increased adipocyte differentiation into mature adipocytes responsible for adiponectin secretion,[52] suggesting that the variant alleles may act to reduce *PTH1R* expression, leading to higher adipocyte differentiation and higher adiponectin levels. *PTH1R* has also been studied extensively in bone marrow, which has been shown to secrete higher levels of adiponectin than white adipose tissue,[58] suggesting that the effect of this locus on adiponectin levels might be mediated by secretion of adiponectin from the bone marrow.

Another example of a nonsynonymous variant representing a potential false lead for causality with adiponectin is rs3087866 (p.Gln299Arg; MAF = 0.21) located within an exon of *DALRD3*, a locus that has also been associated with central adiposity.[36] While the exact function is unknown,

DALRD3 encodes a protein with an anticodon "DALR" binding domain, similar to that of tRNA synthetases. At this locus, however, the strongest colocalized eQTL is for *PRKAR2A*, which encodes a regulatory subunit of protein kinase A. *Prkar2a* knockout mice weigh less than wild-type littermates and are resistant to diet-induced obesity, glucose intolerance, and fatty liver.[59] At the human adiponectin-associated locus, the rs3087866-C allele was associated with decreased adiponectin levels and decreased adipose *PRKAR2A* expression. This observation is consistent with the smaller adipose tissue depots observed in knockout mice[59] and supports the possibility that *PRKAR2A* contributes to the associations with both adiponectin and central adiposity. The other colocalized eQTLs for *AMT* and *NICN1* at this locus were weaker and less clearly relevant to adipose biology.

Exome arrays contain variants with sparse coverage, and trait-associated variants can be located hundreds of kilobases from their target genes. Here, rs10282707 (MAF = 0.38), previously associated with HDL cholesterol,[25] is located within an intron of *SNX13*, sorting nexin 13. This gene belongs to the sorting nexin family, a G protein signaling regulator family of molecules that are involved in intracellular trafficking and regulate G alpha subunits of heterotrimeric G proteins. Located 200 kb downstream of *SNX13*, *HDAC9* (MIM: 606543) encodes histone deacetylase 9, which alters chromosome structure and affects transcription factor access to DNA. *HDAC9* has been shown to be a negative regulator of adipocyte differentiation.[60] Higher levels of *Hdac9* prevented adipocyte differentiation, and knockout of *Hdac9* in mice protected from adipose tissue dysfunction and systemic metabolic disease during high fat feeding.[61] In humans, the allele associated with higher adiponectin and lower HDL cholesterol levels may act by reducing *HDAC9* expression or function. The GWAS data helped guide interpretation of candidate genes at this locus.

Using the context of regional LD and existing adiponectin GWAS data from ADIPOGen[14] is not sufficient for mapping of multiple association signals at a locus. For example, *CDH13* encodes an extracellular cadherin-13 receptor that binds to adiponectin,[62] and variants near *CDH13* are well established to show very strong adiponectin association.[14,19] The strongest adiponectin-associated variant near *CDH13* from the exome array analysis was rs3865188, located near the *CDH13* promoter, although rs3865188 is in low LD ($r^2 = 0.16$) with the lead variant in the genome-wide data, rs12051272.[14] The exome array analysis also identified an adiponectin-associated variant (rs145119400, MAF = 0.005) nearly 1.5 Mb away within *SLC38A8*, and association analysis conditioning on rs145119400 identified yet another signal 260 kb upstream, within an exon of *CDH13* (rs186440718, MAF = 0.003). Neither rs145119400 nor rs186440718 are available in the ADIPOGen consortium data, and rs145119400 is present in only one person in the 1000 Genomes Phase 3 reference panel. Thus, we were not able to determine the number of association signals, nor whether these three variants are all tagging the established *CDH13* association signals, nor whether rs145119400 and *SLC38A8* represent a distinct association signal and candidate gene for adiponectin biology. Future genome-wide association data in larger datasets with dense marker maps will provide valuable opportunities to perform more detailed genomic and fine-mapping analyses to identify potential candidate genes and pathways.

Identification of the gene(s) underlying genetic association signals is imperative to translate associated variants to biological processes. One method that has proven useful for the prediction of candidate functional genes is with the detection of colocalized eQTLs in relevant tissues.[63–65] However, determination of colocalized GWASs and eQTL loci requires accurate identification of the variants most strongly associated with the phenotype and gene expression levels in both sets of data. With the sparse coverage of variants in the exome array, other untested variants in low to moderate LD with the lead exome variant may exhibit stronger trait associations, leading to false identification of a colocalized eQTL or, more likely, missing a colocalized eQTL signal. Larger and more diverse eQTL studies including both sexes and broader ancestry could help identify additional colocalized association signals. While exome array data can be valuable in identifying low-frequency or rare variants present on the array that are often poorly imputed from genotyping arrays, caution should be used in translating association results into candidate functional variants and genes.

Taken together, our results emphasize the value of using exome array analysis for identification of both coding and noncoding signals in discovery of candidate genes relevant for lipid and obesity biology. However, use of genome-wide association data to characterize exome array signals facilitated detection of the LD structure in the association signals, a few of which suggested that more strongly associated variants exist outside exons. As such, caution should be used in the interpretation of results from both exome array and exome-sequencing studies.[66] Future GWASs in larger sample sizes will be valuable to validate these results and extend them to additional loci and genes that influence cardiometabolic traits and diseases.

Data Availability

Summary genetic association results can be found at http://www.thelooslab.com/#data. All other relevant data are in the paper and Supplemental Data.

Supplemental Data

Supplemental Data can be found online at https://doi.org/10.1016/j.ajhg.2019.05.002.

Acknowledgments

The authors thank all investigators, staff members, and study participants for their contributions to all the participating studies.

Funding information for all participating cohorts are provided in the Supplemental Data.

J.B.-J. and T.H. were partially funded by the Novo Nordisk Foundation Center for Basic Metabolic Research, an independent Research Center at the University of Copenhagen. R.S.F. was supported by NHGRI F31 HG009850. T.M.F. was supported by the European Research Council (grant 323195:GLUCOSEGENES-FP7-IDEAS-ERC). H.M.H. was supported by NHLBI T32 HL007055 and T32 HL129982. T.K. was supported by the Novo Nordisk Foundation Center for Protein Research (grants NNF17OC0027594 and NNF14CC0001). T.O.K. was supported by the Danish Council for Independent Research (grant DFF – 6110-00183) and the Novo Nordisk Foundation (grant NNF17OC0026848). C.M.L. is supported by the Li Ka Shing Foundation, WT-SSI/John Fell funds, the NIHR Biomedical Research Centre, Oxford, Widenlife, and NIH (grant 5P50HD028138-27). M.I. McCarthy is a Wellcome Trust Senior Investigator (grant WT098381) and a National Institute of Health Research Senior Investigator, and the views expressed in this article are those of the author(s) and not necessarily those of the NHS, the NIHR, or the Department of Health. J.B. Meigs is supported by NIH K24 DK080140. K.L.M. was supported by NIH R01DK072193 and R01DK093757. D.M.-K. is supported by Dutch Science Organization (ZonMW-VENI Grant 916.14.023). K.E.N. was supported by NIH R01DK089256, R01HD057194, U01HG007416, and R01DK101855 and AHA 13GRNT16490017. C.K.R. was supported by National Institutes of Health (grant 5T32GM67553). S.R. was supported by the Academy of Finland Center of Excellence in Complex Disease Genetics (grant 312062) and the Academy of Finland (grant 285380). V.S. was supported by the Finnish Foundation for Cardiovascular Research. C.N.S. was supported by the American Heart Association Postdoctoral Fellowships 15POST24470131 and 17POST33650016. J.G.W. is supported by U54GM115428 from the National Institute of General Medical Sciences. L.B.L.W. was supported by Wellcome Trust (WT083442AIA). H.Y. was funded by Diabetes UK RD Lawrence fellowship (grant 17/ 0005594). K.L.Y. was supported by KL2TR001109.

Declaration of Interests

This work was conducted prior to M.E.G.'s current affiliation with the National Heart, Lung, and Blood Institute, and, as such, the views expressed in this article do not represent the views of the NHLBI, NIH, or other government entity. D.M.-K. is a part-time clinical research consultant for Metabolon, Inc. M.A.N.'s participation is supported by a consulting contract between Data Tecnica International and the National Institute on Aging, National Institutes of Health. V.S. has participated in a conference trip and received an honorarium sponsored by Novo Nordisk.

Received: February 26, 2019
Accepted: April 30, 2019
Published: June 6, 2019

Web Resources

EC-DEPICT, https://github.com/RebeccaFine/obesity-ec-depict
Illumina HumanExome Beadchip Array, https://genome.sph.umich.edu/wiki/Exome_Chip_Design
OMIM, https://www.omim.org/
Pascal, https://www2.unil.ch/cbg/index.php?title=Pascal
PhenoScanner, http://www.phenoscanner.medschl.cam.ac.uk

References

1. Azrad, M., Gower, B.A., Hunter, G.R., and Nagy, T.R. (2013). Racial differences in adiponectin and leptin in healthy premenopausal women. Endocrine *43*, 586–592.
2. Wang, X., Bao, W., Liu, J., Ouyang, Y.Y., Wang, D., Rong, S., Xiao, X., Shan, Z.L., Zhang, Y., Yao, P., and Liu, L.G. (2013). Inflammatory markers and risk of type 2 diabetes: a systematic review and meta-analysis. Diabetes Care *36*, 166–175.
3. Breitfeld, J., Stumvoll, M., and Kovacs, P. (2012). Genetics of adiponectin. Biochimie *94*, 2157–2163.
4. Goldstein, B.J., Scalia, R.G., and Ma, X.L. (2009). Protective vascular and myocardial effects of adiponectin. Nat. Clin. Pract. Cardiovasc. Med. *6*, 27–35.
5. Povel, C.M., Boer, J.M., and Feskens, E.J. (2011). Shared genetic variance between the features of the metabolic syndrome: heritability studies. Mol. Genet. Metab. *104*, 666–669.
6. Henneman, P., Aulchenko, Y.S., Frants, R.R., Zorkoltseva, I.V., Zillikens, M.C., Frolich, M., Oostra, B.A., van Dijk, K.W., and van Duijn, C.M. (2010). Genetic architecture of plasma adiponectin overlaps with the genetics of metabolic syndrome-related traits. Diabetes Care *33*, 908–913.
7. Au Yeung, S.L., and Schooling, C.M. (2018). Adiponectin and coronary artery disease risk: A bi-directional Mendelian randomization study. Int. J. Cardiol. *268*, 222–226.
8. Yaghootkar, H., Lamina, C., Scott, R.A., Dastani, Z., Hivert, M.F., Warren, L.L., Stancáková, A., Buxbaum, S.G., Lyytikäinen, L.P., Henneman, P., et al.; GENESIS Consortium; and RISC Consortium (2013). Mendelian randomization studies do not support a causal role for reduced circulating adiponectin levels in insulin resistance and type 2 diabetes. Diabetes *62*, 3589–3598.
9. Mente, A., Meyre, D., Lanktree, M.B., Heydarpour, M., Davis, A.D., Miller, R., Gerstein, H., Hegele, R.A., Yusuf, S., Anand, S.S.; SHARE Investigators; and SHARE-AP Investigators (2013). Causal relationship between adiponectin and metabolic traits: a Mendelian randomization study in a multiethnic population. PLoS ONE *8*, e66808.
10. Gao, H., Fall, T., van Dam, R.M., Flyvbjerg, A., Zethelius, B., Ingelsson, E., and Hägg, S. (2013). Evidence of a causal relationship between adiponectin levels and insulin sensitivity: a Mendelian randomization study. Diabetes *62*, 1338–1344.
11. Xia, J.Y., Sun, K., Hepler, C., Ghaben, A.L., Gupta, R.K., An, Y.A., Holland, W.L., Morley, T.S., Adams, A.C., Gordillo, R., et al. (2018). Acute loss of adipose tissue-derived adiponectin triggers immediate metabolic deterioration in mice. Diabetologia *61*, 932–941.
12. Holland, W.L., Miller, R.A., Wang, Z.V., Sun, K., Barth, B.M., Bui, H.H., Davis, K.E., Bikman, B.T., Halberg, N., Rutkowski, J.M., et al. (2011). Receptor-mediated activation of ceramidase activity initiates the pleiotropic actions of adiponectin. Nat. Med. *17*, 55–63.
13. Sattar, N., and Nelson, S.M. (2008). Adiponectin, diabetes, and coronary heart disease in older persons: unraveling the paradox. J. Clin. Endocrinol. Metab. *93*, 3299–3301.
14. Dastani, Z., Hivert, M.F., Timpson, N., Perry, J.R., Yuan, X., Scott, R.A., Henneman, P., Heid, I.M., Kizer, J.R., Lyytikäinen, L.P., et al.; DIAGRAM+ Consortium; MAGIC Consortium;

GLGC Investigators; MuTHER Consortium; DIAGRAM Consortium; GIANT Consortium; Global B Pgen Consortium; Procardis Consortium; MAGIC investigators; and GLGC Consortium (2012). Novel loci for adiponectin levels and their influence on type 2 diabetes and metabolic traits: a multi-ethnic meta-analysis of 45,891 individuals. PLoS Genet. *8*, e1002607.

15. Nawrocki, A.R., Rajala, M.W., Tomas, E., Pajvani, U.B., Saha, A.K., Trumbauer, M.E., Pang, Z., Chen, A.S., Ruderman, N.B., Chen, H., et al. (2006). Mice lacking adiponectin show decreased hepatic insulin sensitivity and reduced responsiveness to peroxisome proliferator-activated receptor gamma agonists. J. Biol. Chem. *281*, 2654–2660.
16. Chuang, L.M., Chiu, Y.F., Sheu, W.H., Hung, Y.J., Ho, L.T., Grove, J., Rodriguez, B., Quertermous, T., Chen, Y.D., Hsiung, C.A., Tai, T.Y.; and Stanford Asia-Pacific Program of Hypertension and Insulin Resistance Study Group (2004). Biethnic comparisons of autosomal genomic scan for loci linked to plasma adiponectin in populations of Chinese and Japanese origin. J. Clin. Endocrinol. Metab. *89*, 5772–5778.
17. Comuzzie, A.G., Funahashi, T., Sonnenberg, G., Martin, L.J., Jacob, H.J., Black, A.E., Maas, D., Takahashi, M., Kihara, S., Tanaka, S., et al. (2001). The genetic basis of plasma variation in adiponectin, a global endophenotype for obesity and the metabolic syndrome. J. Clin. Endocrinol. Metab. *86*, 4321–4325.
18. Lindsay, R.S., Funahashi, T., Krakoff, J., Matsuzawa, Y., Tanaka, S., Kobes, S., Bennett, P.H., Tataranni, P.A., Knowler, W.C., and Hanson, R.L. (2003). Genome-wide linkage analysis of serum adiponectin in the Pima Indian population. Diabetes *52*, 2419–2425.
19. Wu, Y., Gao, H., Li, H., Tabara, Y., Nakatochi, M., Chiu, Y.F., Park, E.J., Wen, W., Adair, L.S., Borja, J.B., et al. (2014). A meta-analysis of genome-wide association studies for adiponectin levels in East Asians identifies a novel locus near WDR11-FGFR2. Hum. Mol. Genet. *23*, 1108–1119.
20. Richards, J.B., Waterworth, D., O'Rahilly, S., Hivert, M.F., Loos, R.J., Perry, J.R., Tanaka, T., Timpson, N.J., Semple, R.K., Soranzo, N., et al.; GIANT Consortium (2009). A genome-wide association study reveals variants in ARL15 that influence adiponectin levels. PLoS Genet. *5*, e1000768.
21. Mahajan, A., Wessel, J., Willems, S.M., Zhao, W., Robertson, N.R., Chu, A.Y., Gan, W., Kitajima, H., Taliun, D., Rayner, N.W., et al.; ExomeBP Consortium; MAGIC Consortium; and GIANT Consortium (2018). Refining the accuracy of validated target identification through coding variant fine-mapping in type 2 diabetes. Nat. Genet. *50*, 559–571.
22. Feng, S., Liu, D., Zhan, X., Wing, M.K., and Abecasis, G.R. (2014). RAREMETAL: fast and powerful meta-analysis for rare variants. Bioinformatics *30*, 2828–2829.
23. Zhan, X., Hu, Y., Li, B., Abecasis, G.R., and Liu, D.J. (2016). RVTESTS: an efficient and comprehensive tool for rare variant association analysis using sequence data. Bioinformatics *32*, 1423–1426.
24. Winkler, T.W., Day, F.R., Croteau-Chonka, D.C., Wood, A.R., Locke, A.E., Mägi, R., Ferreira, T., Fall, T., Graff, M., Justice, A.E., et al.; Genetic Investigation of Anthropometric Traits (GIANT) Consortium (2014). Quality control and conduct of genome-wide association meta-analyses. Nat. Protoc. *9*, 1192–1212.
25. Liu, D.J., Peloso, G.M., Yu, H., Butterworth, A.S., Wang, X., Mahajan, A., Saleheen, D., Emdin, C., Alam, D., Alves, A.C., et al.; Charge Diabetes Working Group; EPIC-InterAct Consortium; EPIC-CVD Consortium; GOLD Consortium; and VA Million Veteran Program (2017). Exome-wide association study of plasma lipids in >300,000 individuals. Nat. Genet. *49*, 1758–1766.
26. Turcot, V., Lu, Y., Highland, H.M., Schurmann, C., Justice, A.E., Fine, R.S., Bradfield, J.P., Esko, T., Giri, A., Graff, M., et al.; CHD Exome+ Consortium; EPIC-CVD Consortium; ExomeBP Consortium; Global Lipids Genetic Consortium; GoT2D Genes Consortium; EPIC InterAct Consortium; INTERVAL Study; ReproGen Consortium; T2D-Genes Consortium; MAGIC Investigators; and Understanding Society Scientific Group (2018). Protein-altering variants associated with body mass index implicate pathways that control energy intake and expenditure in obesity. Nat. Genet. *50*, 26–41.
27. Liu, D.J., Peloso, G.M., Zhan, X., Holmen, O.L., Zawistowski, M., Feng, S., Nikpay, M., Auer, P.L., Goel, A., Zhang, H., et al. (2014). Meta-analysis of gene-level tests for rare variant association. Nat. Genet. *46*, 200–204.
28. Winkler, T.W., Kutalik, Z., Gorski, M., Lottaz, C., Kronenberg, F., and Heid, I.M. (2015). EasyStrata: evaluation and visualization of stratified genome-wide association meta-analysis data. Bioinformatics *31*, 259–261.
29. Wu, M.C., Lee, S., Cai, T., Li, Y., Boehnke, M., and Lin, X. (2011). Rare-variant association testing for sequencing data with the sequence kernel association test. Am. J. Hum. Genet. *89*, 82–93.
30. Price, A.L., Kryukov, G.V., de Bakker, P.I., Purcell, S.M., Staples, J., Wei, L.J., and Sunyaev, S.R. (2010). Pooled association tests for rare variants in exon-resequencing studies. Am. J. Hum. Genet. *86*, 832–838.
31. Purcell, S.M., Moran, J.L., Fromer, M., Ruderfer, D., Solovieff, N., Roussos, P., O'Dushlaine, C., Chambert, K., Bergen, S.E., Kähler, A., et al. (2014). A polygenic burden of rare disruptive mutations in schizophrenia. Nature *506*, 185–190.
32. Kiezun, A., Garimella, K., Do, R., Stitziel, N.O., Neale, B.M., McLaren, P.J., Gupta, N., Sklar, P., Sullivan, P.F., Moran, J.L., et al. (2012). Exome sequencing and the genetic basis of complex traits. Nat. Genet. *44*, 623–630.
33. Aschard, H., Vilhjálmsson, B.J., Joshi, A.D., Price, A.L., and Kraft, P. (2015). Adjusting for heritable covariates can bias effect estimates in genome-wide association studies. Am. J. Hum. Genet. *96*, 329–339.
34. Day, F.R., Loh, P.R., Scott, R.A., Ong, K.K., and Perry, J.R. (2016). A Robust Example of Collider Bias in a Genetic Association Study. Am. J. Hum. Genet. *98*, 392–393.
35. Willer, C.J., Speliotes, E.K., Loos, R.J., Li, S., Lindgren, C.M., Heid, I.M., Berndt, S.I., Elliott, A.L., Jackson, A.U., Lamina, C., et al.; Wellcome Trust Case Control Consortium; and Genetic Investigation of ANthropometric Traits Consortium (2009). Six new loci associated with body mass index highlight a neuronal influence on body weight regulation. Nat. Genet. *41*, 25–34.
36. Justice, A.E., Karaderi, T., Highland, H.M., Young, K.L., Graff, M., Lu, Y., Turcot, V., Auer, P.L., Fine, R.S., Guo, X., et al.; CHD Exome+ Consortium; Cohorts for Heart and Aging Research in Genomic Epidemiology (CHARGE) Consortium; EPIC-CVD Consortium; ExomeBP Consortium; Global Lipids Genetic Consortium; GoT2D Genes Consortium; InterAct; ReproGen Consortium; T2D-Genes Consortium; and MAGIC Investigators (2019). Protein-coding variants implicate novel genes related to lipid homeostasis contributing to body-fat distribution. Nat. Genet. *51*, 452–469.

37. Wheeler, E., Leong, A., Liu, C.T., Hivert, M.F., Strawbridge, R.J., Podmore, C., Li, M., Yao, J., Sim, X., Hong, J., et al.; EPIC-CVD Consortium; EPIC-InterAct Consortium; and Lifelines Cohort Study (2017). Impact of common genetic determinants of Hemoglobin A1c on type 2 diabetes risk and diagnosis in ancestrally diverse populations: A trans-ethnic genome-wide meta-analysis. PLoS Med. *14*, e1002383.
38. Manning, A.K., Hivert, M.F., Scott, R.A., Grimsby, J.L., Bouatia-Naji, N., Chen, H., Rybin, D., Liu, C.T., Bielak, L.F., Prokopenko, I., et al.; DIAbetes Genetics Replication And Meta-analysis (DIAGRAM) Consortium; and Multiple Tissue Human Expression Resource (MUTHER) Consortium (2012). A genome-wide approach accounting for body mass index identifies genetic variants influencing fasting glycemic traits and insulin resistance. Nat. Genet. *44*, 659–669.
39. Scott, R.A., Lagou, V., Welch, R.P., Wheeler, E., Montasser, M.E., Luan, J., Mägi, R., Strawbridge, R.J., Rehnberg, E., Gustafsson, S., et al.; DIAbetes Genetics Replication and Meta-analysis (DIAGRAM) Consortium (2012). Large-scale association analyses identify new loci influencing glycemic traits and provide insight into the underlying biological pathways. Nat. Genet. *44*, 991–1005.
40. Scott, R.A., Scott, L.J., Mägi, R., Marullo, L., Gaulton, K.J., Kaakinen, M., Pervjakova, N., Pers, T.H., Johnson, A.D., Eicher, J.D., et al.; DIAbetes Genetics Replication And Meta-analysis (DIAGRAM) Consortium (2017). An Expanded Genome-Wide Association Study of Type 2 Diabetes in Europeans. Diabetes *66*, 2888–2902.
41. Civelek, M., Wu, Y., Pan, C., Raulerson, C.K., Ko, A., He, A., Tilford, C., Saleem, N.K., Stančáková, A., Scott, L.J., et al. (2017). Genetic regulation of adipose gene expression and cardio-metabolic traits. Am. J. Hum. Genet. *100*, 428–443.
42. GTEx Consortium (2013). The Genotype-Tissue Expression (GTEx) project. Nat. Genet. *45*, 580–585.
43. Pers, T.H., Karjalainen, J.M., Chan, Y., Westra, H.J., Wood, A.R., Yang, J., Lui, J.C., Vedantam, S., Gustafsson, S., Esko, T., et al.; Genetic Investigation of ANthropometric Traits (GIANT) Consortium (2015). Biological interpretation of genome-wide association studies using predicted gene functions. Nat. Commun. *6*, 5890.
44. Marouli, E., Graff, M., Medina-Gomez, C., Lo, K.S., Wood, A.R., Kjaer, T.R., Fine, R.S., Lu, Y., Schurmann, C., Highland, H.M., et al.; EPIC-InterAct Consortium; CHD Exome+ Consortium; ExomeBP Consortium; T2D-Genes Consortium; GoT2D Genes Consortium; Global Lipids Genetics Consortium; ReproGen Consortium; and MAGIC Investigators (2017). Rare and low-frequency coding variants alter human adult height. Nature *542*, 186–190.
45. Lamparter, D., Marbach, D., Rueedi, R., Kutalik, Z., and Bergmann, S. (2016). Fast and Rigorous Computation of Gene and Pathway Scores from SNP-Based Summary Statistics. PLoS Comput. Biol. *12*, e1004714.
46. Moayyeri, A., Hammond, C.J., Valdes, A.M., and Spector, T.D. (2013). Cohort Profile: TwinsUK and healthy ageing twin study. Int. J. Epidemiol. *42*, 76–85.
47. Boyd, A., Golding, J., Macleod, J., Lawlor, D.A., Fraser, A., Henderson, J., Molloy, L., Ness, A., Ring, S., and Davey Smith, G. (2013). Cohort Profile: the 'children of the 90s'–the index offspring of the Avon Longitudinal Study of Parents and Children. Int. J. Epidemiol. *42*, 111–127.
48. Pain, O., Dudbridge, F., and Ronald, A. (2018). Are your covariates under control? How normalization can re-introduce covariate effects. Eur. J. Hum. Genet. *26*, 1194–1201.
49. Hivert, M.F., Manning, A.K., McAteer, J.B., Florez, J.C., Dupuis, J., Fox, C.S., O'Donnell, C.J., Cupples, L.A., and Meigs, J.B. (2008). Common variants in the adiponectin gene (ADIPOQ) associated with plasma adiponectin levels, type 2 diabetes, and diabetes-related quantitative traits: the Framingham Offspring Study. Diabetes *57*, 3353–3359.
50. Jee, S.H., Sull, J.W., Lee, J.E., Shin, C., Park, J., Kimm, H., Cho, E.Y., Shin, E.S., Yun, J.E., Park, J.W., et al. (2010). Adiponectin concentrations: a genome-wide association study. Am. J. Hum. Genet. *87*, 545–552.
51. Pickrell, J.K., Berisa, T., Liu, J.Z., Ségurel, L., Tung, J.Y., and Hinds, D.A. (2016). Detection and interpretation of shared genetic influences on 42 human traits. Nat. Genet. *48*, 709–717.
52. Fan, Y., Hanai, J.I., Le, P.T., Bi, R., Maridas, D., DeMambro, V., Figueroa, C.A., Kir, S., Zhou, X., Mannstadt, M., et al. (2017). Parathyroid Hormone Directs Bone Marrow Mesenchymal Cell Fate. Cell Metab. *25*, 661–672.
53. Lundbäck, V., Kulyte, A., Strawbridge, R.J., Ryden, M., Arner, P., Marcus, C., and Dahlman, I. (2018). FAM13A and POM121C are candidate genes for fasting insulin: functional follow-up analysis of a genome-wide association study. Diabetologia *61*, 1112–1123.
54. London, E., Nesterova, M., and Stratakis, C.A. (2017). Acute vs chronic exposure to high fat diet leads to distinct regulation of PKA. J. Mol. Endocrinol. *59*, 1–12.
55. Chu, A.Y., Deng, X., Fisher, V.A., Drong, A., Zhang, Y., Feitosa, M.F., Liu, C.T., Weeks, O., Choh, A.C., Duan, Q., et al. (2017). Multiethnic genome-wide meta-analysis of ectopic fat depots identifies loci associated with adipocyte development and differentiation. Nat. Genet. *49*, 125–130.
56. Lee, M.J., and Fried, S.K. (2014). The glucocorticoid receptor, not the mineralocorticoid receptor, plays the dominant role in adipogenesis and adipokine production in human adipocytes. Int. J. Obes. *38*, 1228–1233.
57. Tikhonenko, I., Magidson, V., Gräf, R., Khodjakov, A., and Koonce, M.P. (2013). A kinesin-mediated mechanism that couples centrosomes to nuclei. Cell. Mol. Life Sci. *70*, 1285–1296.
58. Cawthorn, W.P., Scheller, E.L., Learman, B.S., Parlee, S.D., Simon, B.R., Mori, H., Ning, X., Bree, A.J., Schell, B., Broome, D.T., et al. (2014). Bone marrow adipose tissue is an endocrine organ that contributes to increased circulating adiponectin during caloric restriction. Cell Metab. *20*, 368–375.
59. London, E., Nesterova, M., Sinaii, N., Szarek, E., Chanturiya, T., Mastroyannis, S.A., Gavrilova, O., and Stratakis, C.A. (2014). Differentially regulated protein kinase A (PKA) activity in adipose tissue and liver is associated with resistance to diet-induced obesity and glucose intolerance in mice that lack PKA regulatory subunit type IIα. Endocrinology *155*, 3397–3408.
60. Chatterjee, T.K., Idelman, G., Blanco, V., Blomkalns, A.L., Piegore, M.G., Jr., Weintraub, D.S., Kumar, S., Rajsheker, S., Manka, D., Rudich, S.M., et al. (2011). Histone deacetylase 9 is a negative regulator of adipogenic differentiation. J. Biol. Chem. *286*, 27836–27847.
61. Chatterjee, T.K., Basford, J.E., Knoll, E., Tong, W.S., Blanco, V., Blomkalns, A.L., Rudich, S., Lentsch, A.B., Hui, D.Y., and Weintraub, N.L. (2014). HDAC9 knockout mice are protected from adipose tissue dysfunction and systemic metabolic disease during high-fat feeding. Diabetes *63*, 176–187.

62. Williams, A.S., Kasahara, D.I., Verbout, N.G., Fedulov, A.V., Zhu, M., Si, H., Wurmbrand, A.P., Hug, C., Ranscht, B., and Shore, S.A. (2012). Role of the adiponectin binding protein, T-cadherin (Cdh13), in allergic airways responses in mice. PLoS ONE *7*, e41088.
63. Conde, L., Bracci, P.M., Richardson, R., Montgomery, S.B., and Skibola, C.F. (2013). Integrating GWAS and expression data for functional characterization of disease-associated SNPs: an application to follicular lymphoma. Am. J. Hum. Genet. *92*, 126–130.
64. Albert, F.W., and Kruglyak, L. (2015). The role of regulatory variation in complex traits and disease. Nat. Rev. Genet. *16*, 197–212.
65. Brænne, I., Civelek, M., Vilne, B., Di Narzo, A., Johnson, A.D., Zhao, Y., Reiz, B., Codoni, V., Webb, T.R., Foroughi Asl, H., et al.; Leducq Consortium CAD Genomics‡ (2015). Prediction of Causal Candidate Genes in Coronary Artery Disease Loci. Arterioscler. Thromb. Vasc. Biol. *35*, 2207–2217.
66. Huyghe, J.R., Jackson, A.U., Fogarty, M.P., Buchkovich, M.L., Stančáková, A., Stringham, H.M., Sim, X., Yang, L., Fuchsberger, C., Cederberg, H., et al. (2013). Exome array analysis identifies new loci and low-frequency variants influencing insulin processing and secretion. Nat. Genet. *45*, 197–201.

The American Journal of Human Genetics, Volume *105*

Supplemental Data

Exome-Derived Adiponectin-Associated Variants Implicate Obesity and Lipid Biology

Cassandra N. Spracklen, Tugce Karaderi, Hanieh Yaghootkar, Claudia Schurmann, Rebecca S. Fine, Zoltan Kutalik, Michael H. Preuss, Yingchang Lu, Laura B.L. Wittemans, Linda S. Adair, Matthew Allison, Najaf Amin, Paul L. Auer, Traci M. Bartz, Matthias Blüher, Michael Boehnke, Judith B. Borja, Jette Bork-Jensen, Linda Broer, Daniel I. Chasman, Yii-Der Ida Chen, Paraskevi Chirstofidou, Ayse Demirkan, Cornelia M. van Duijn, Mary F. Feitosa, Melissa E. Garcia, Mariaelisa Graff, Harald Grallert, Niels Grarup, Xiuqing Guo, Jeffrey Haesser, Torben Hansen, Tamara B. Harris, Heather M. Highland, Jaeyoung Hong, M. Arfan Ikram, Erik Ingelsson, Rebecca Jackson, Pekka Jousilahti, Mika Kähönen, Jorge R. Kizer, Peter Kovacs, Jennifer Kriebel, Markku Laakso, Leslie A. Lange, Terho Lehtimäki, Jin Li, Ruifang Li-Gao, Lars Lind, Jian'an Luan, Leo-Pekka Lyytikäinen, Stuart MacGregor, David A. Mackey, Anubha Mahajan, Massimo Mangino, Satu Männistö, Mark I. McCarthy, Barbara McKnight, Carolina Medina-Gomez, James B. Meigs, Sophie Molnos, Dennis Mook-Kanamori, Andrew P. Morris, Renee de Mutsert, Mike A. Nalls, Ivana Nedeljkovic, Kari E. North, Craig E. Pennell, Aruna D. Pradhan, Michael A. Province, Olli T. Raitakari, Chelsea K. Raulerson, Alex P. Reiner, Paul M. Ridker, Samuli Ripatti, Neil Roberston, Jerome I. Rotter, Veikko Salomaa, America A. Sandoval-Zárate, Colleen M. Sitlani, Tim D. Spector, Konstantin Strauch, Michael Stumvoll, Kent D. Taylor, Betina Thuesen, Anke Tönjes, Andre G. Uitterlinden, Cristina Venturini, Mark Walker, Carol A. Wang, Shuai Wang, Nicholas J. Wareham, Sara M. Willems, Ko Willems van Dijk, James G. Wilson, Ying Wu, Jie Yao, Kristin L. Young, Claudia Langenberg, Timothy M. Frayling, Tuomas O. Kilpeläinen, Cecilia M. Lindgren, Ruth J.F. Loos, and Karen L. Mohlke

SUPPLEMENTAL FIGURES

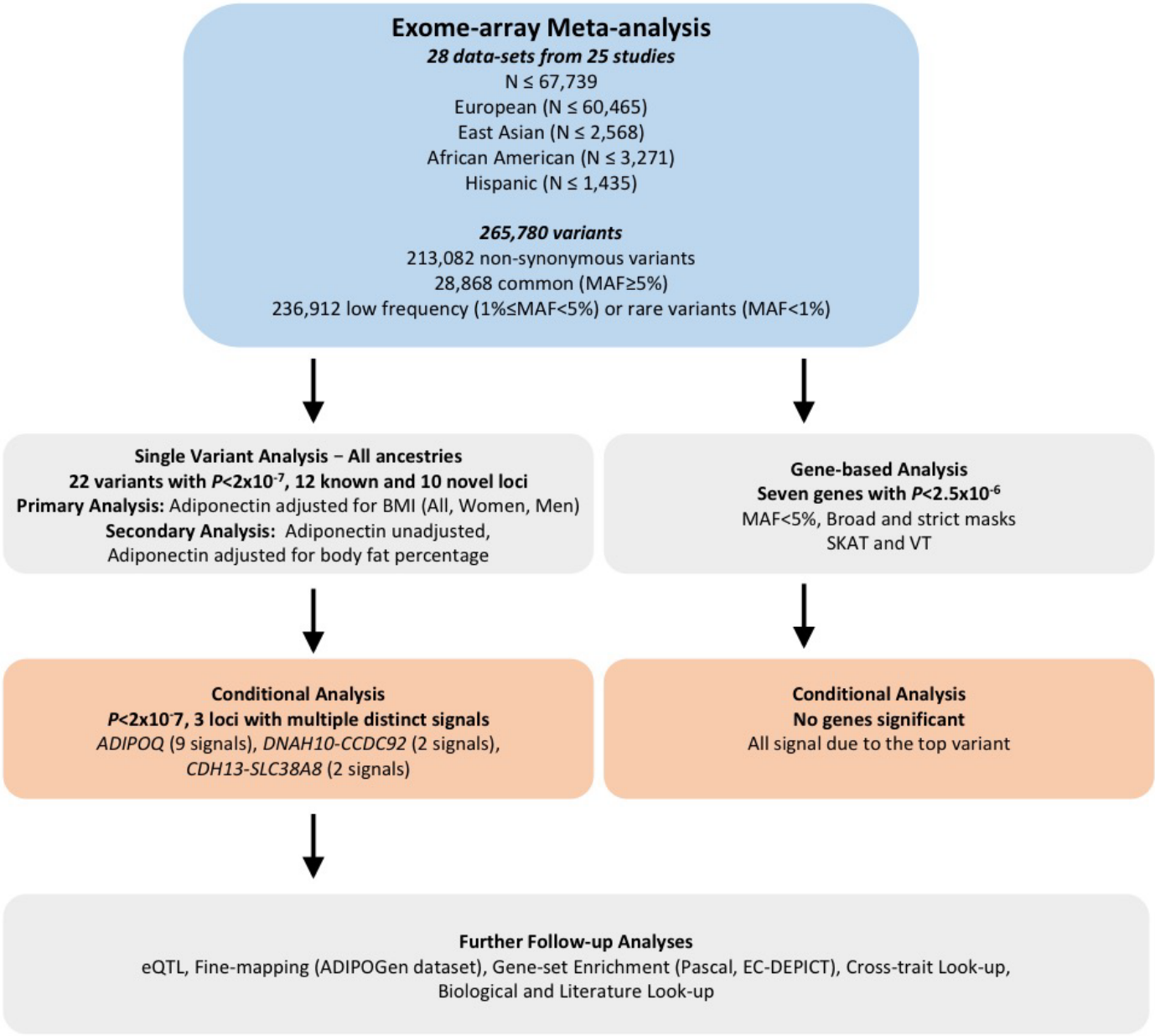

Figure S1. Workflow for the adiponectin exome-array meta-analysis and follow-up analyses.
MAF, minor allele frequency; BMI, body mass index.

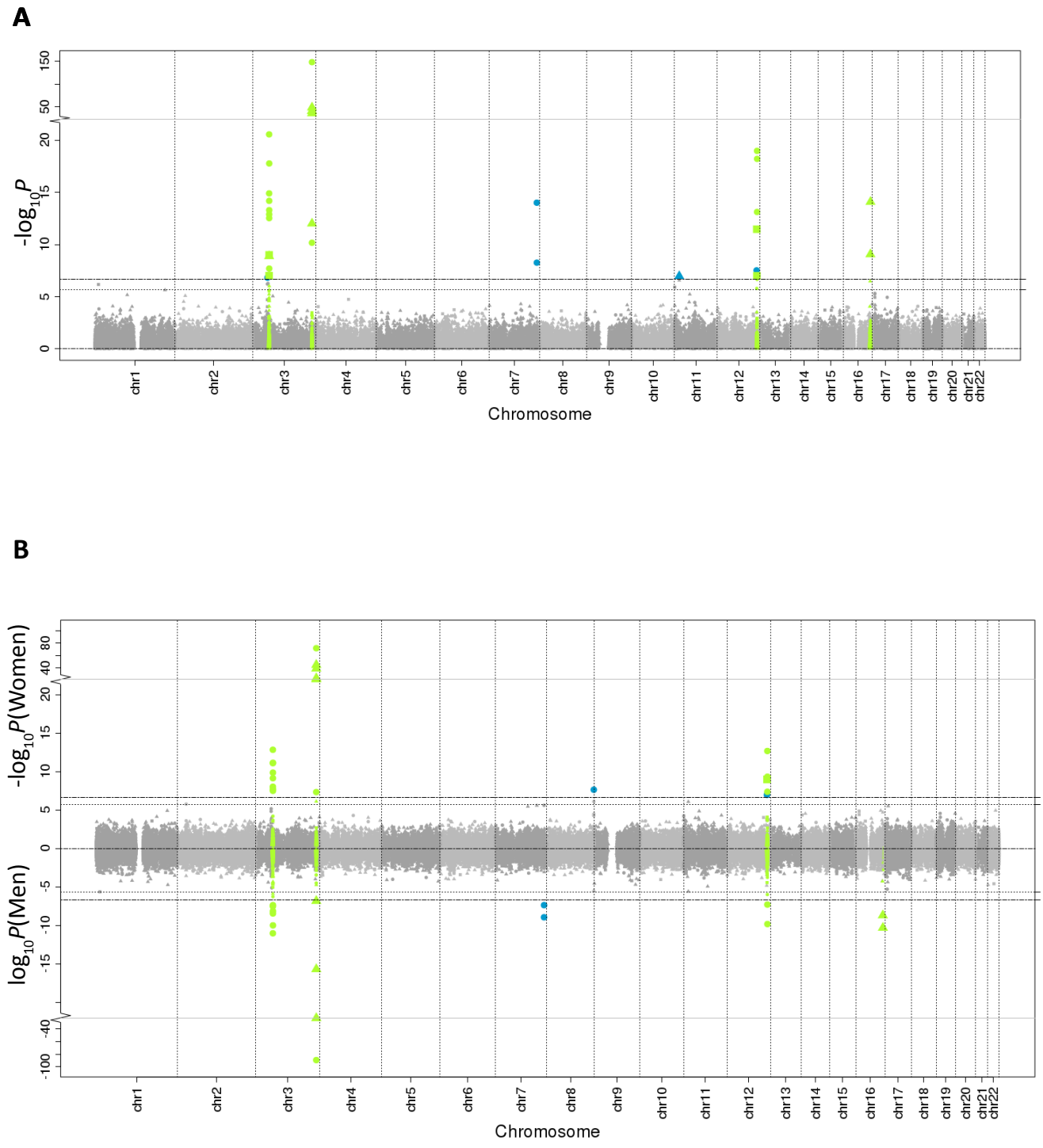

Figure S2. Adiponectin association results for models unadjusted for BMI or fat percentage. (A) Manhattan plot showing the exome-wide variants in the adiponectin unadjusted analysis [X-axis: Chromosome number; Y-axis: $-\log_{10}(P)$ for the all ancestries sex-combined additive model]. Green highlighted variants show the previously identified loci that also achieved $P<2\times10^{-6}$ in this dataset. Horizontal lines mark *P*-value thresholds 2×10^{-7} (top; array-wide significance level) and 2×10^{-6} (suggestive; bottom). (B) Miami plot showing the exome-wide variants in sex-specific analyses [X-axis: Chromosome number; Top panel y-axis: $-\log_{10}P$(Women); Bottom panel y-axis: $-\log_{10}P$(Men) for the all ancestries additive model]. Green highlighted variants show the previously identified loci that also achieved $P<2\times10^{-6}$ in each dataset. Horizontal lines mark *P*-value thresholds 2×10^{-7} (array-wide significance level) and 2×10^{-6} (suggestive). Circles, triangles, squares correspond to MAF≥0.05, MAF<0.01 and MAF<0.05, respectively. Blue symbols represent novel associations achieving $P<2\times10^{-7}$.

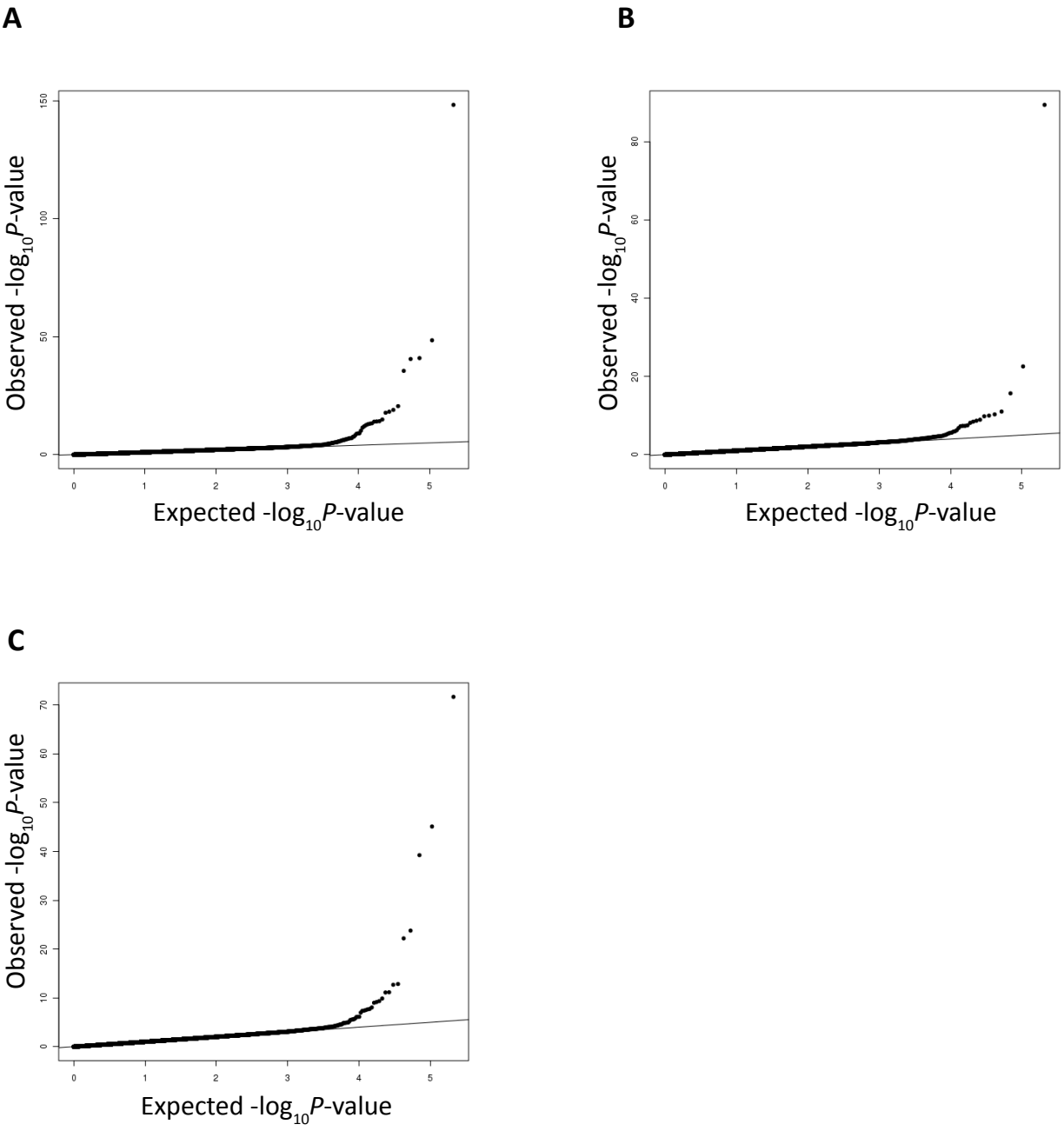

Figure S3. QQ plots of the exome-wide variants in the adiponectin unadjusted analysis
[X-axis: Expected $-\log_{10}(P)$; Y-axis: Observed $-\log_{10}(P)$]. (A) All ancestries sex-combined additive model; (B) All ancestries men-specific additive model; (C) All ancestries women-specific additive model.

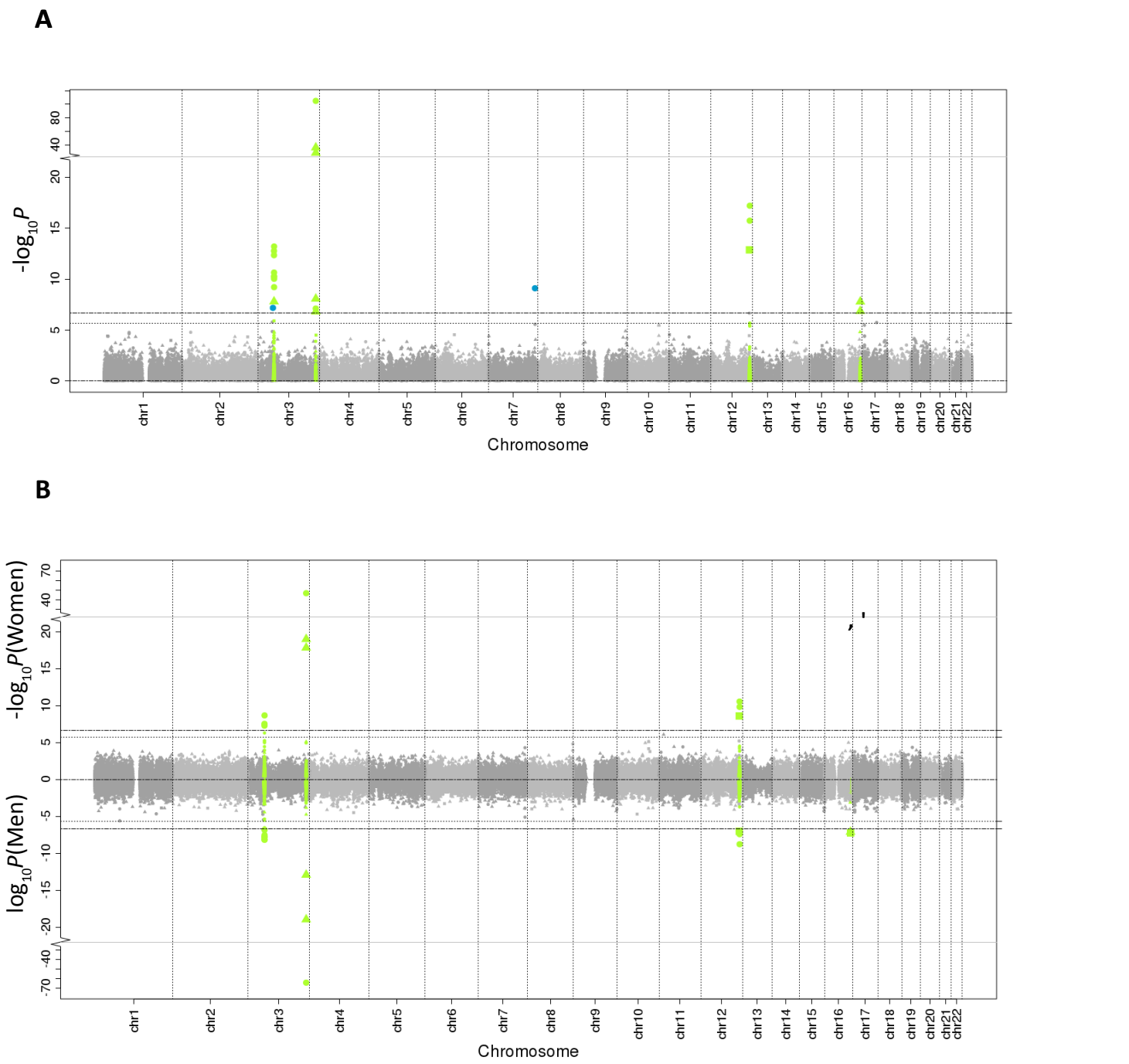

Figure S4. Adiponectin associaiton results for models adjusted for fat percentage.
(A) Manhattan plot showing the exome-wide variants in the adiponectin adjusted for fat percentage analysis [X-axis: Chromosome number; Y-axis: $-\log_{10}(P)$ for the all ancestries sex-combined additive model]. Green highlighted variants show the previously identified loci that also achieved $P<2\times10^{-6}$ in this dataset. Horizontal lines mark *P*-value thresholds 2×10^{-7} (top; array-wide significance level) and 2×10^{-6} (suggestive; bottom). (B) Miami plot showing the exome-wide variants in sex-specific analyses [X-axis: Chromosome number; Top panel y-axis: $-\log_{10}P$(Women); Bottom panel y-axis: $-\log_{10}P$(Men) for the all ancestries additive model]. Green highlighted variants show the previously identified loci that also achieved $P<2\times10^{-6}$ in each dataset. Horizontal lines mark *P*-value thresholds 2×10^{-7} (array-wide significance level) and 2×10^{-6} (suggestive). Circles, triangles, squares correspond to MAF≥0.05, MAF<0.01 and MAF<0.05, respectively. Blue symbols represent novel associations with $P<2\times10^{-7}$.

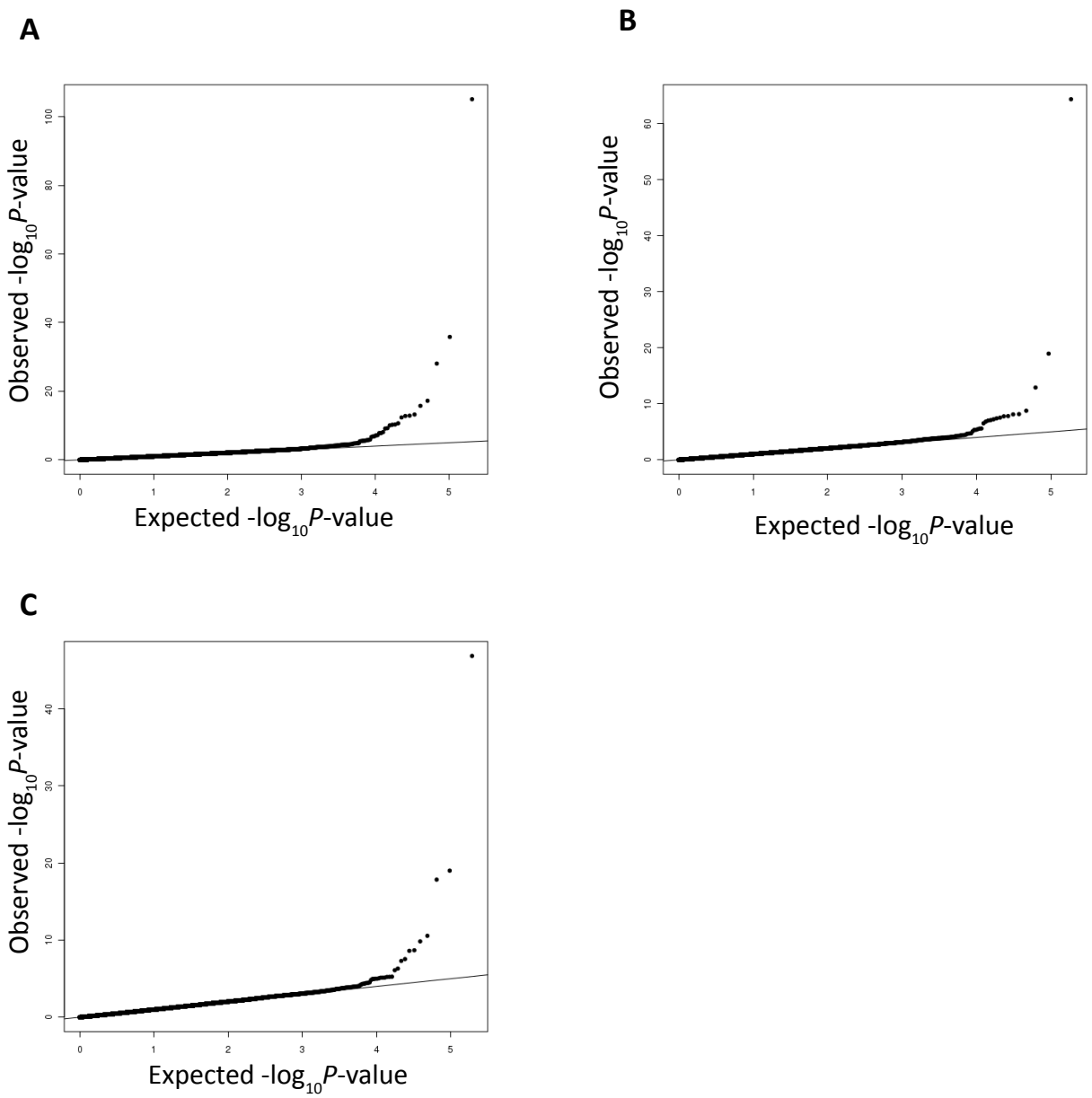

Figure S5. QQ plots showing the exome-wide variants in the adiponectin adjusted for fat percent analysis [X-axis: Expected –$\log_{10}$(P); Y-axis: Observed -$\log_{10}$(P)]. (A) All ancestries sex-combined additive model; (B) All ancestries men-specific additive model; (C) All ancestries women-specific additive model.

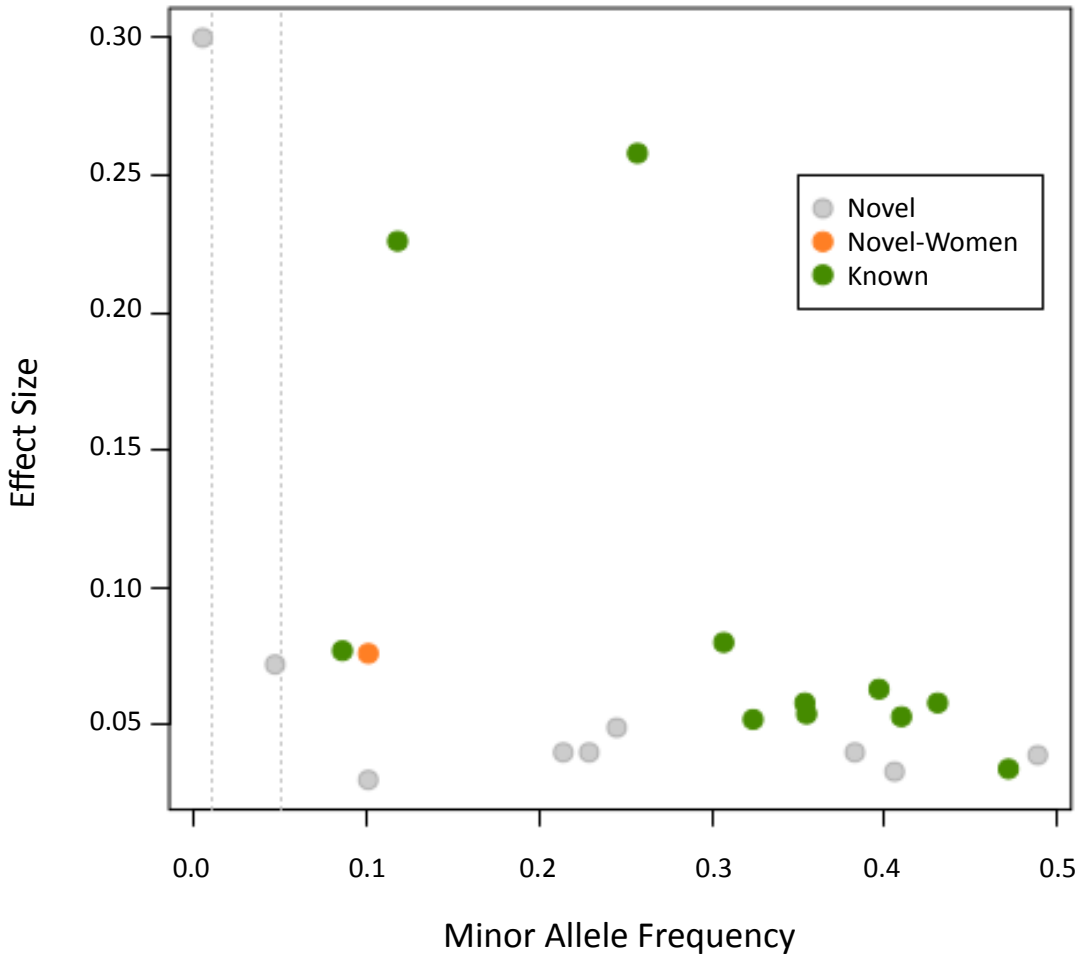

Figure S6. Effect size vs. minor allele frequency (MAF) for variants in the primary adiponectin analysis [X-axis: MAF; Y-axis: effect size for the all ancestries, sex-combined and women-specific additive model]. Gray, orange, and green variants show the novel and previously identified loci that also achieved $P<2x10^{-7}$ in the combined and women-specific analyses as labeled. Vertical lines mark MAF=0.01 and MAF=0.05.

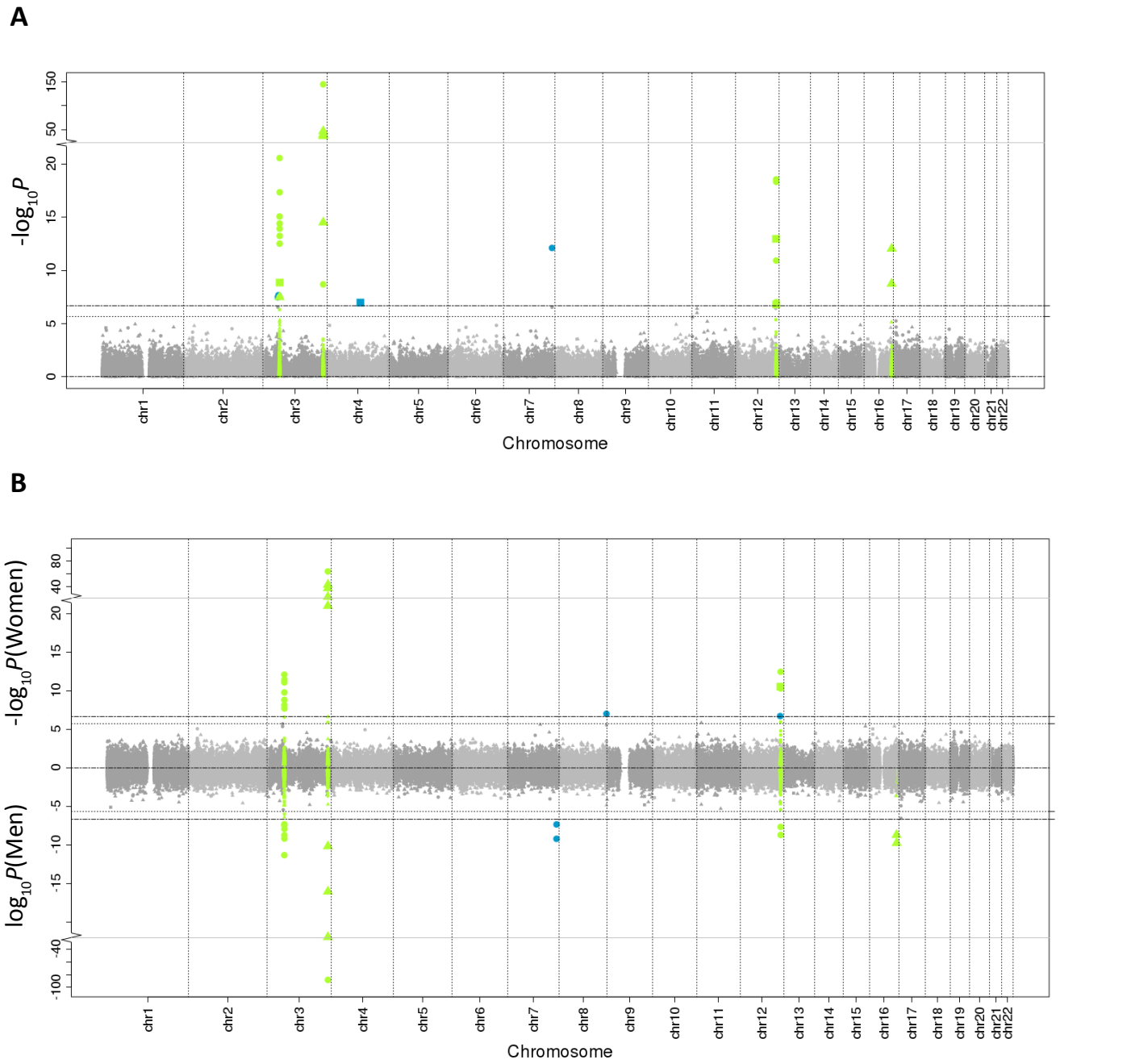

Figure S7. Adiponectin associaiton results for models adjusted for BMI.
(A) Manhattan plot showing the exome-wide variants in the adiponectin adjusted for body mass index analysis [X-axis: Chromosome number; Y-axis: $-\log_{10}(P)$ for the all ancestries sex-combined additive model]. Green highlighted variants show the previously identified loci that also achieved $P<2\times10^{-6}$ in this dataset. Horizontal lines mark *P*-value thresholds 2×10^{-7} (top; array-wide significance level) and 2×10^{-6} (suggestive; bottom). (B) Miami plot showing the exome-wide variants in sex-specific analyses [X-axis: Chromosome number; Top panel y-axis: $-\log_{10}(P_{WOMEN})$; Bottom panel y-axis: $-\log_{10}(P_{MEN})$ for the all ancestries additive model]. Green highlighted variants show the previously identified loci that also achieved $P<2\times10^{-6}$ in each dataset. Horizontal lines mark *P*-value thresholds 2×10^{-7} (array-wide significance level) and 2×10^{-6} (suggestive). Circles, triangles, squares correspond to MAF≥0.05, MAF<0.01 and MAF<0.05, respectively. Blue symbols represent novel associations wtih $P<2\times10^{-7}$.

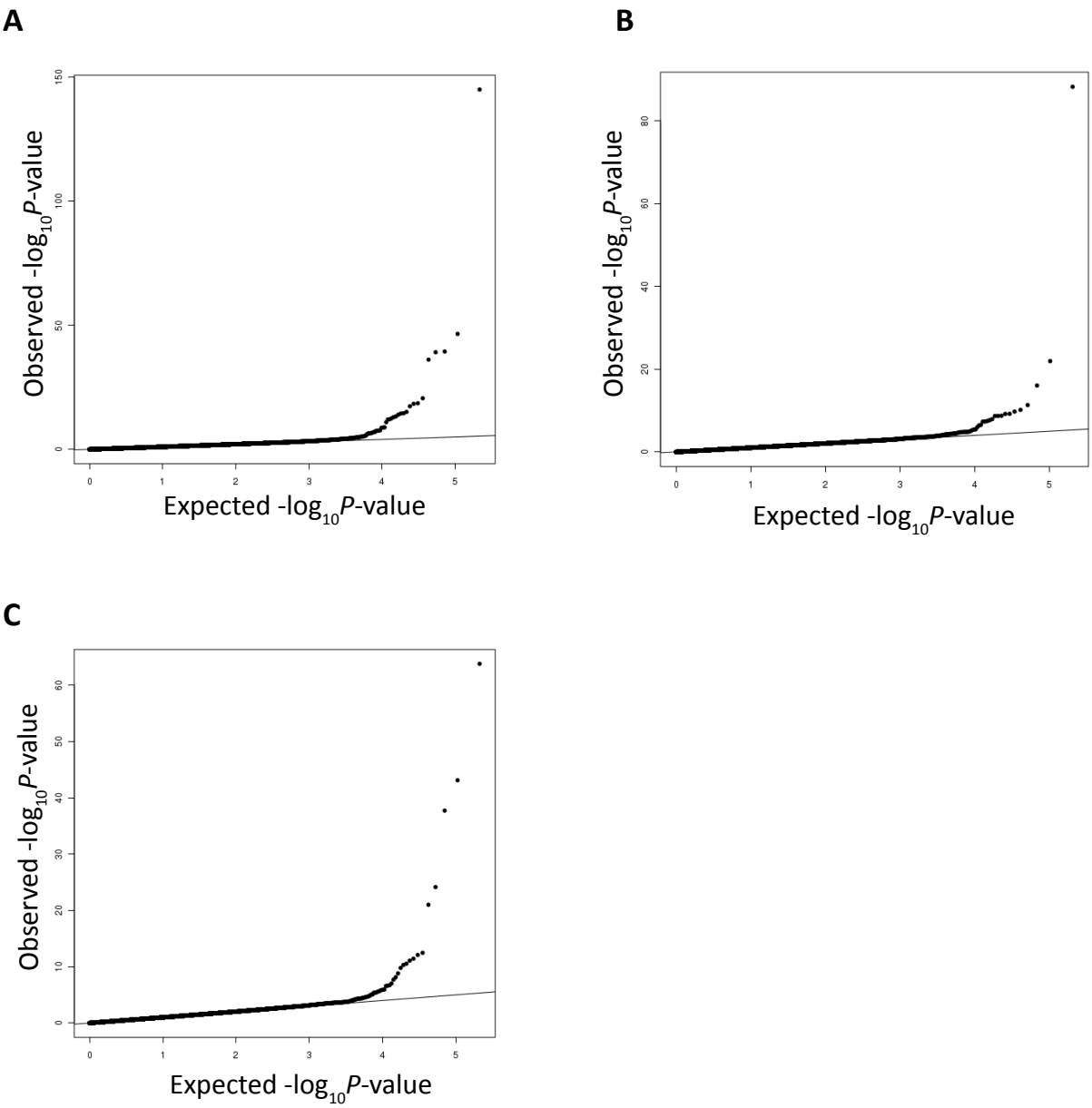

Figure S8. QQ plots showing the exome-wide variants in the adiponectin adjusted for BMI analysis [X-axis: Expected –log10(P); Y-axis: Observed -log10(P)]. (A) All ancestries sex-combined additive model; (B) All ancestries men-specific additive model; (C) All ancestries women-specific additive model.

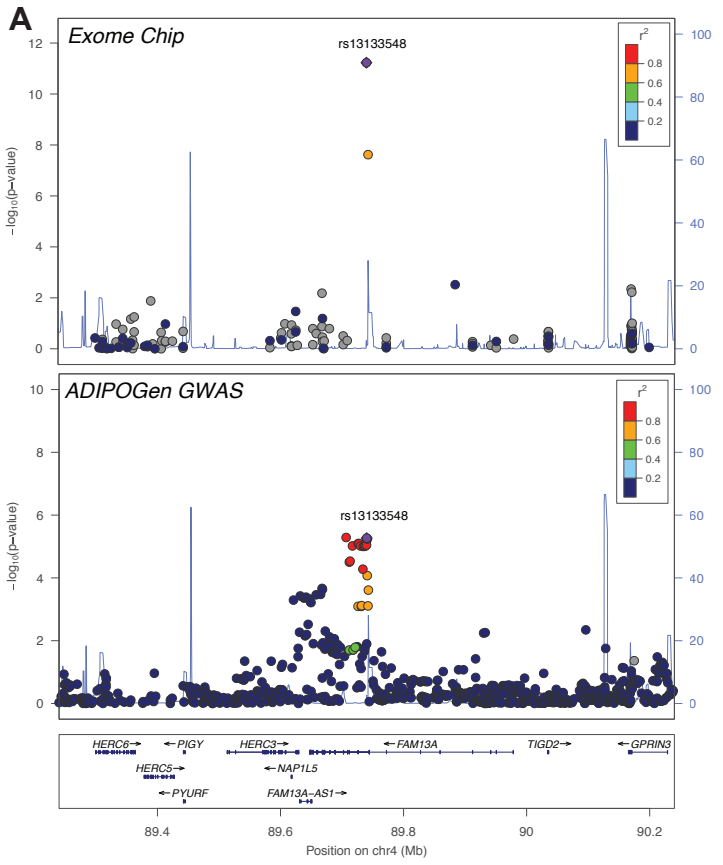
A
Exome Chip
rs13133548
ADIPOGen GWAS
rs13133548
HERC6
PIGY
HERC3
FAM13A
TIGD2
GPRIN3
HERC5
NAP1L5
PYURF
FAM13A-AS1
89.4
89.6
89.8
90
90.2
Position on chr4 (Mb)
−log10(p-value)
Recombination rate (cM/Mb)

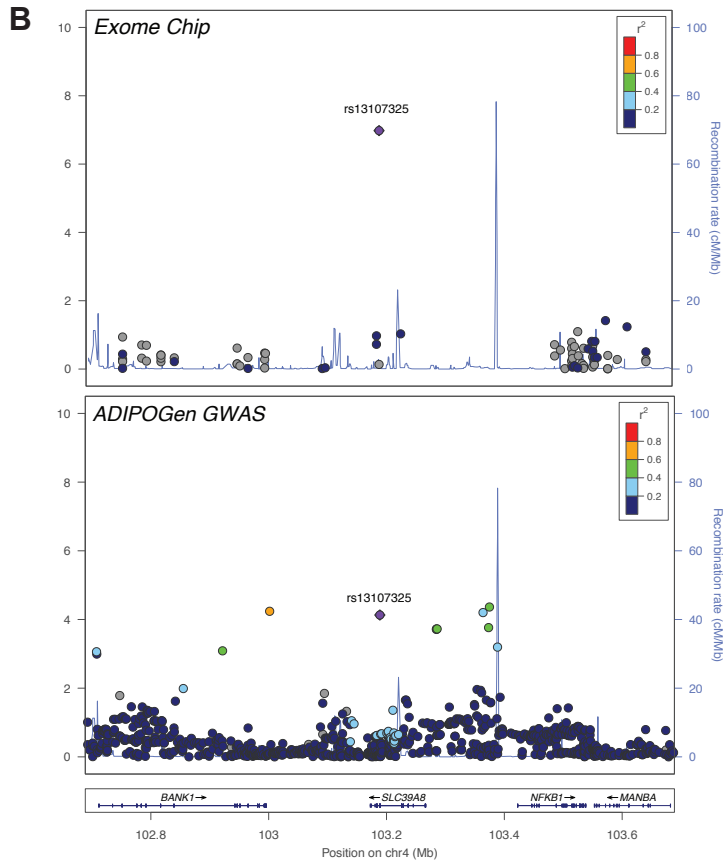
B
Exome Chip
rs13107325
ADIPOGen GWAS
rs13107325
BANK1
SLC39A8
NFKB1
MANBA
102.8
103
103.2
103.4
103.6
Position on chr4 (Mb)
Recombination rate (cM/Mb)

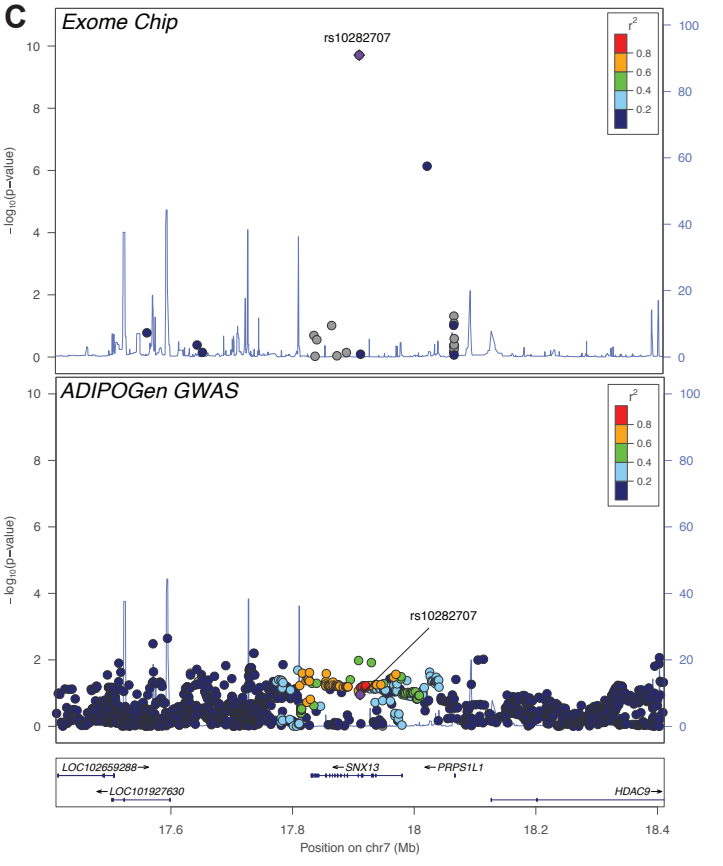
C
Exome Chip
rs10282707
ADIPOGen GWAS
rs10282707
LOC102659288
SNX13
PRPS1L1
LOC101927630
HDAC9
17.6
17.8
18
18.2
18.4
Position on chr7 (Mb)
−log10(p-value)

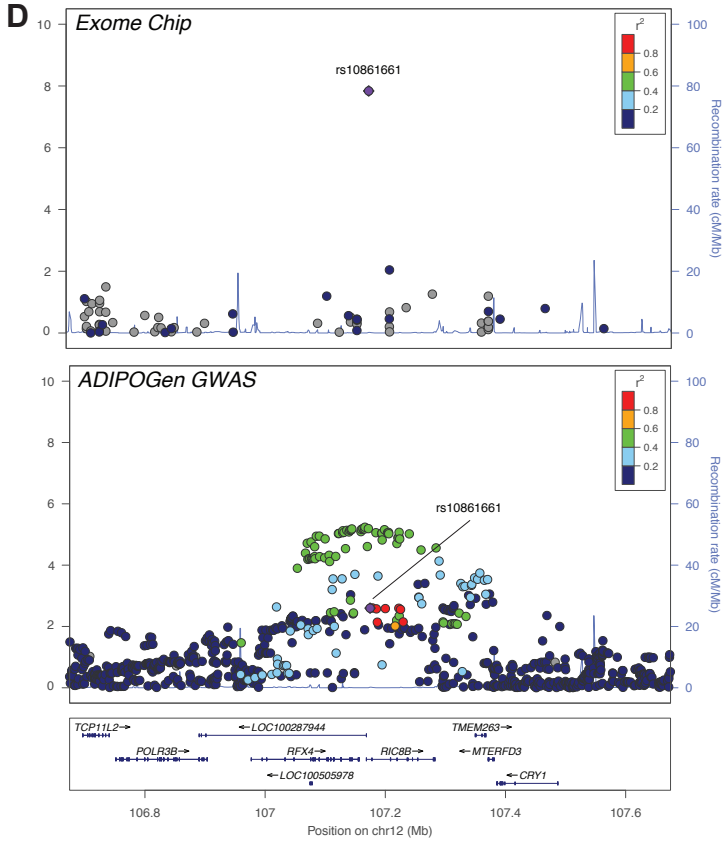
D
Exome Chip
rs10861661
ADIPOGen GWAS
rs10861661
TCP11L2
LOC100287944
TMEM263
POLR3B
RFX4
RIC8B
MTERFD3
LOC100505978
CRY1
106.8
107
107.2
107.4
107.6
Position on chr12 (Mb)
Recombination rate (cM/Mb)

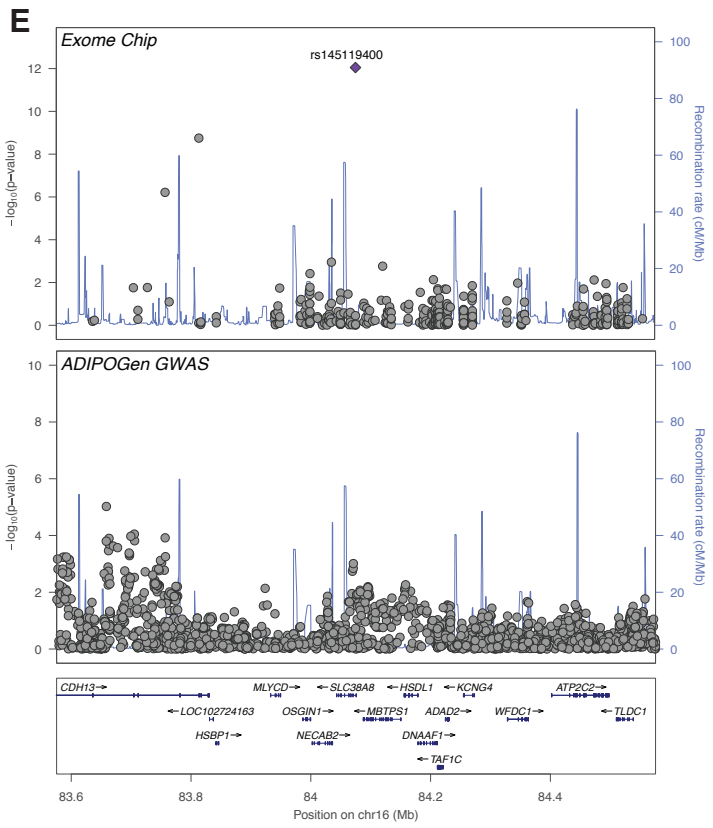

Figure S9. Plots of five previously unreported adiponectin-associated loci in sex-combined exome-wide meta-analysis.

A) *FAM13A*, B) *SLC39A8*, C) *SNX13*, D) *RIC8B*, and E) *SLC38A8*. The upper plots show the current exome-wide meta-analysis, and the lower plots show the genome-wide ADIPOGen consortium meta-analysis from Dastani, et al., 2012. In E, rs145119400 was not included in the ADIPOGen consortium meta-analysis. Each point represents a variant in the meta-analysis, plotted with P-value (on a -log10 scale) on the y-axis and genomic position (hg19) on the x-axis. In each plot, the index variant identified in the exome chip meta-analysis is represented in purple, and the color of all other variants indicate the LD with the index variant in European ancestry haplotypes from the 1000 Genome Phase 3 reference panel. In A, C, and D, the lead variant from the exome-wide analysis may not be the best representative of the adiponectin-associated signal.

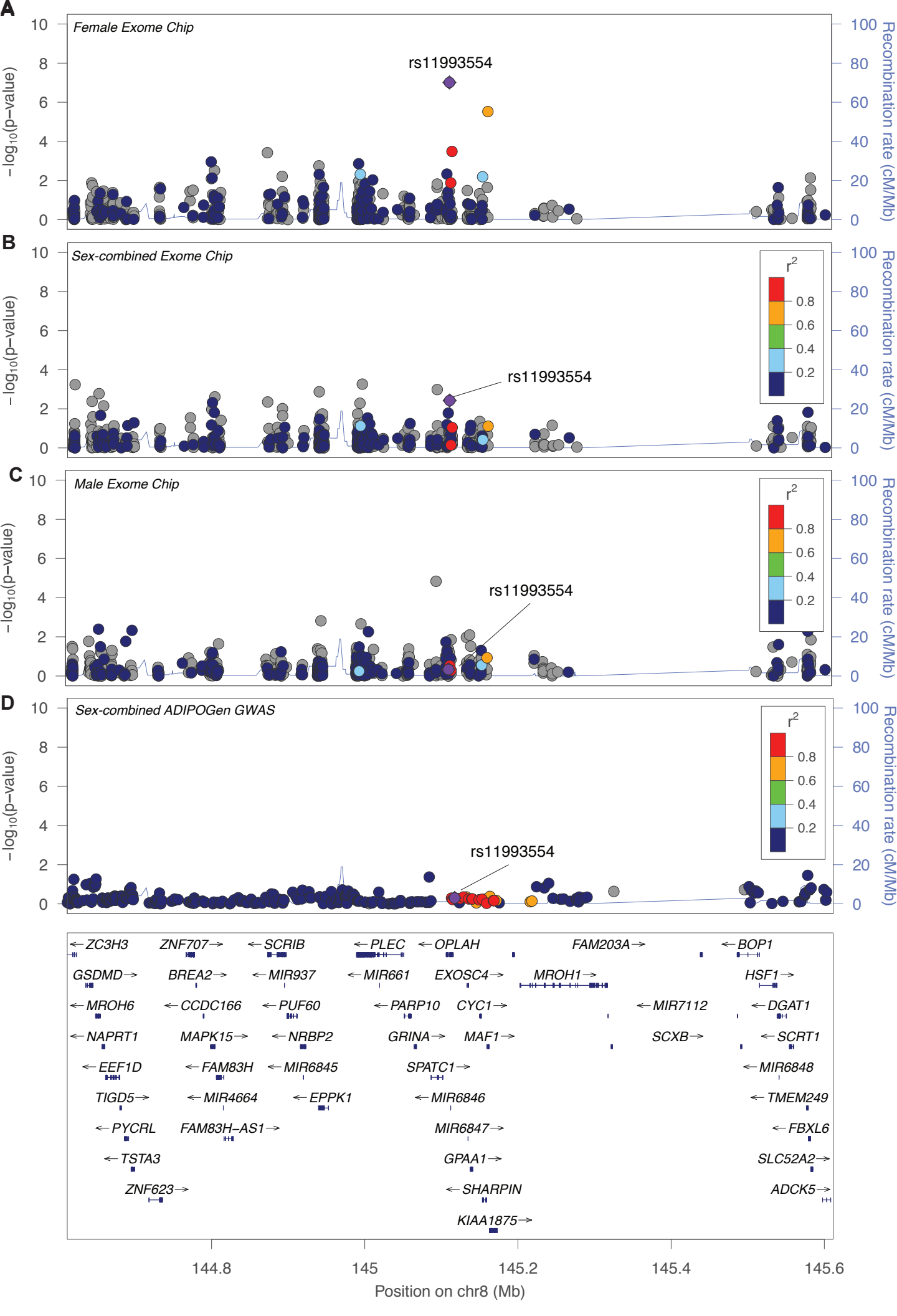
A
Female Exome Chip
rs11993554
B
Sex-combined Exome Chip
rs11993554
C
Male Exome Chip
rs11993554
D
Sex-combined ADIPOGen GWAS
rs11993554
−log10(p−value)
Recombination rate (cM/Mb)
r2
0.8
0.6
0.4
0.2
ZC3H3
ZNF707
SCRIB
PLEC
OPLAH
FAM203A
BOP1
GSDMD
BREA2
MIR937
MIR661
EXOSC4
MROH1
HSF1
MROH6
CCDC166
PUF60
PARP10
CYC1
MIR7112
DGAT1
NAPRT1
MAPK15
NRBP2
GRINA
MAF1
SCXB
SCRT1
EEF1D
FAM83H
MIR6845
SPATC1
MIR6848
TIGD5
MIR4664
EPPK1
MIR6846
TMEM249
PYCRL
FAM83H−AS1
MIR6847
FBXL6
TSTA3
GPAA1
SLC52A2
ZNF623
SHARPIN
ADCK5
KIAA1875
144.8
145
145.2
145.4
145.6
Position on chr8 (Mb)

Figure S10. **Plot of novel adiponectin-associated OPLAH only observed in females**. A) Females only from exome-wide meta-analysis, B) Sex-combined results from exome-wide meta-analysis, C) Males only from exome-wide meta-analysis, and D) Sex-combined genome-wide ADIPOGen meta-analysis. Each point represents a variant in the meta-analysis, plotted with P-value (on a -log10 scale) on the y-axis and genomic position (hg19) on the x-axis. In each plot, the index variant identified in the exome chip meta-analysis is represented in purple, and the color of all other variants indicate the LD with the index variant in European ancestry haplotypes from the 1000 Genome Phase 3 reference panel. Sex-specific data were not available from the ADIPOGen consortium meta-analysis.

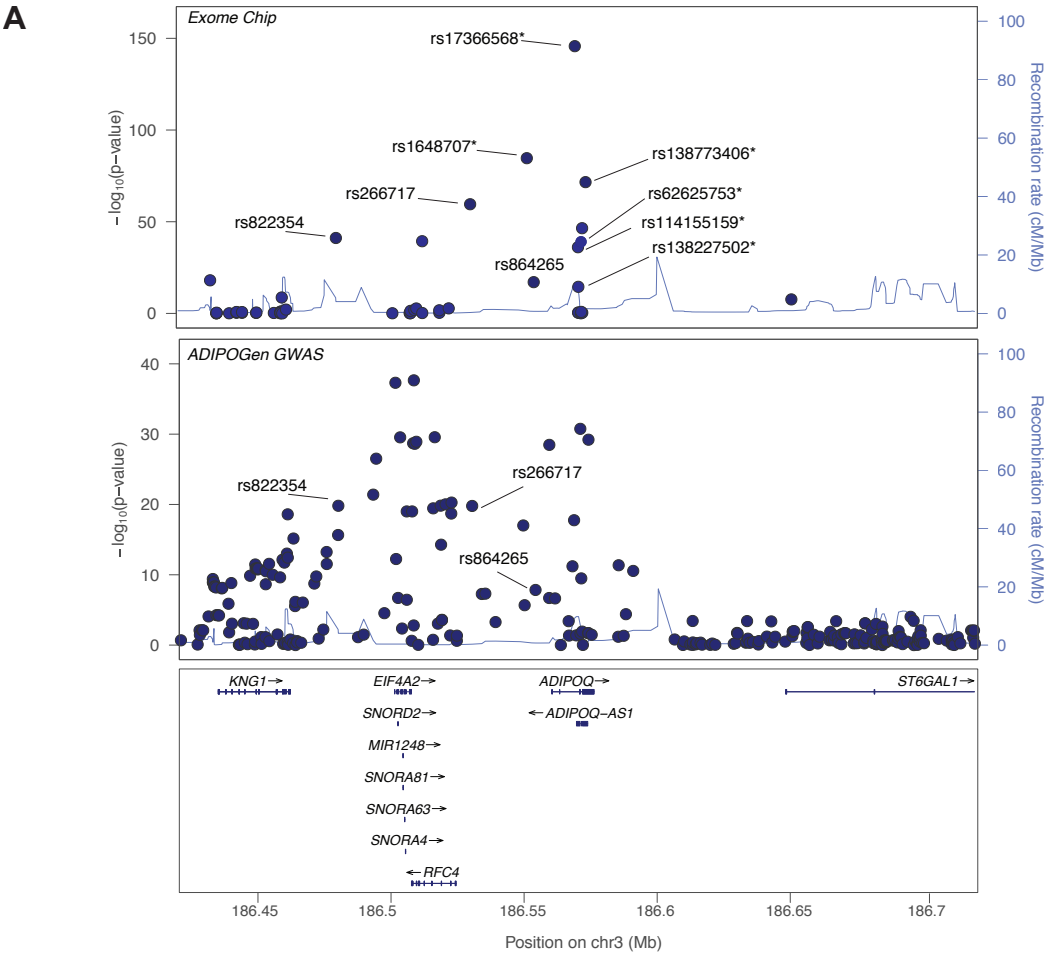
A
Exome Chip
rs17366568*
rs1648707*
rs138773406*
rs266717
rs62625753*
rs822354
rs114155159*
rs138227502*
rs864265
ADIPOGen GWAS
rs822354
rs266717
rs864265
KNG1
EIF4A2
ADIPOQ
ST6GAL1
SNORD2
ADIPOQ-AS1
MIR1248
SNORA81
SNORA63
SNORA4
RFC4
186.45
186.5
186.55
186.6
186.65
186.7
Position on chr3 (Mb)
– log10(p–value)
Recombination rate (cM/Mb)

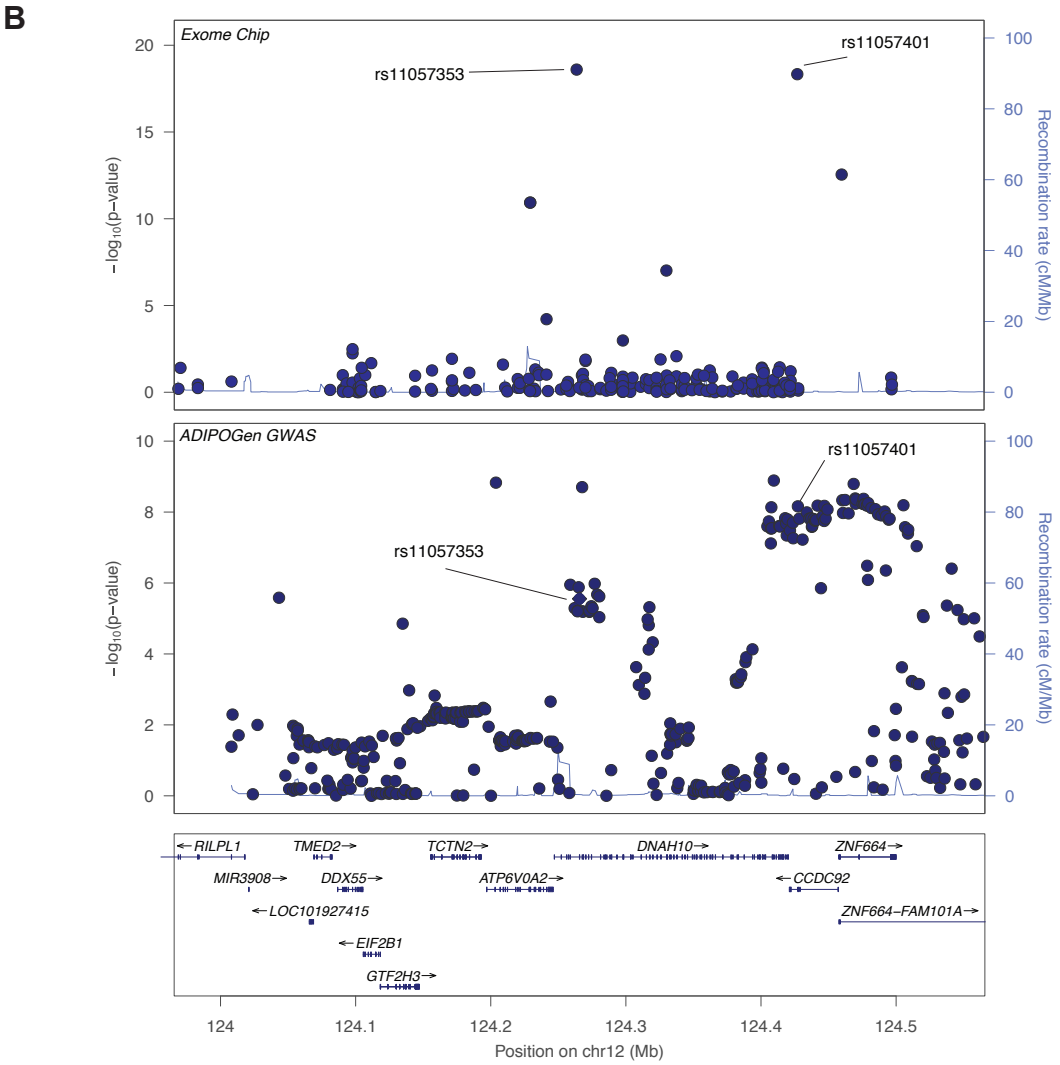
B
Exome Chip
rs11057401
rs11057353
ADIPOGen GWAS
rs11057401
rs11057353
RILPL1
TMED2
TCTN2
DNAH10
ZNF664
MIR3908
DDX55
ATP6V0A2
CCDC92
LOC101927415
ZNF664–FAM101A
EIF2B1
GTF2H3
124
124.1
124.2
124.3
124.4
124.5
Position on chr12 (Mb)
– log10(p–value)
Recombination rate (cM/Mb)

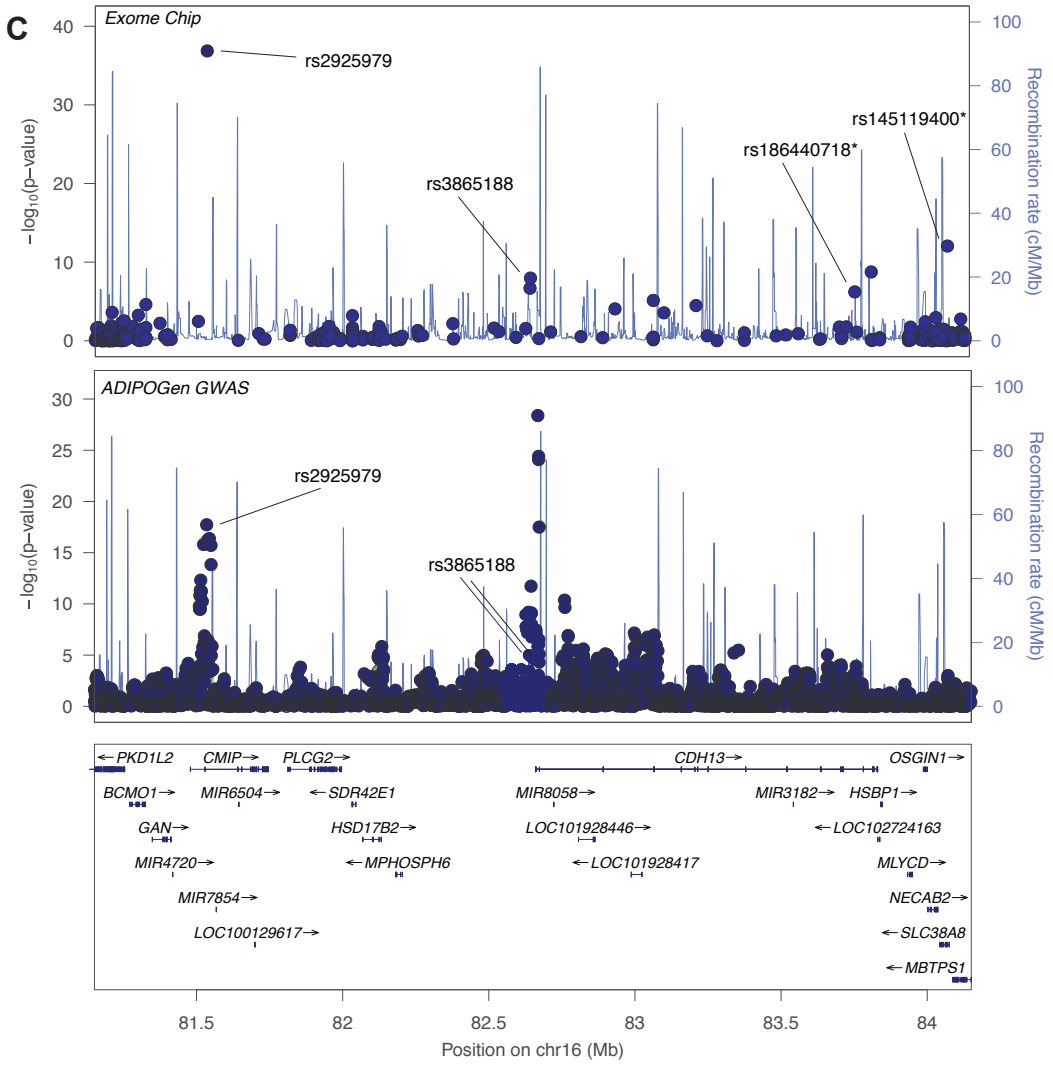

Figure S11. **Three adiponectin loci exhibit multiple distinct association signals.** A) ADIPOQ with nine exome-wide association signals, B) DNAH10-CCDC92 with two exome-wide association signals, and C) CDH13-region with four exome-wide association signals. Each point represents a variant in the meta-analysis, plotted with P-value (on a -log10 scale) on the y-axis and genomic position (hg19) on the x-axis. Asterisks (*) indicate variants identified as a distinct association signal in the Exome Chip analysis but were not present in the ADIPOGen data. Given that many noncoding variants were not tested in this exome-wide analysis, the number of signals and lead variants may differ in genome-wide analyses..

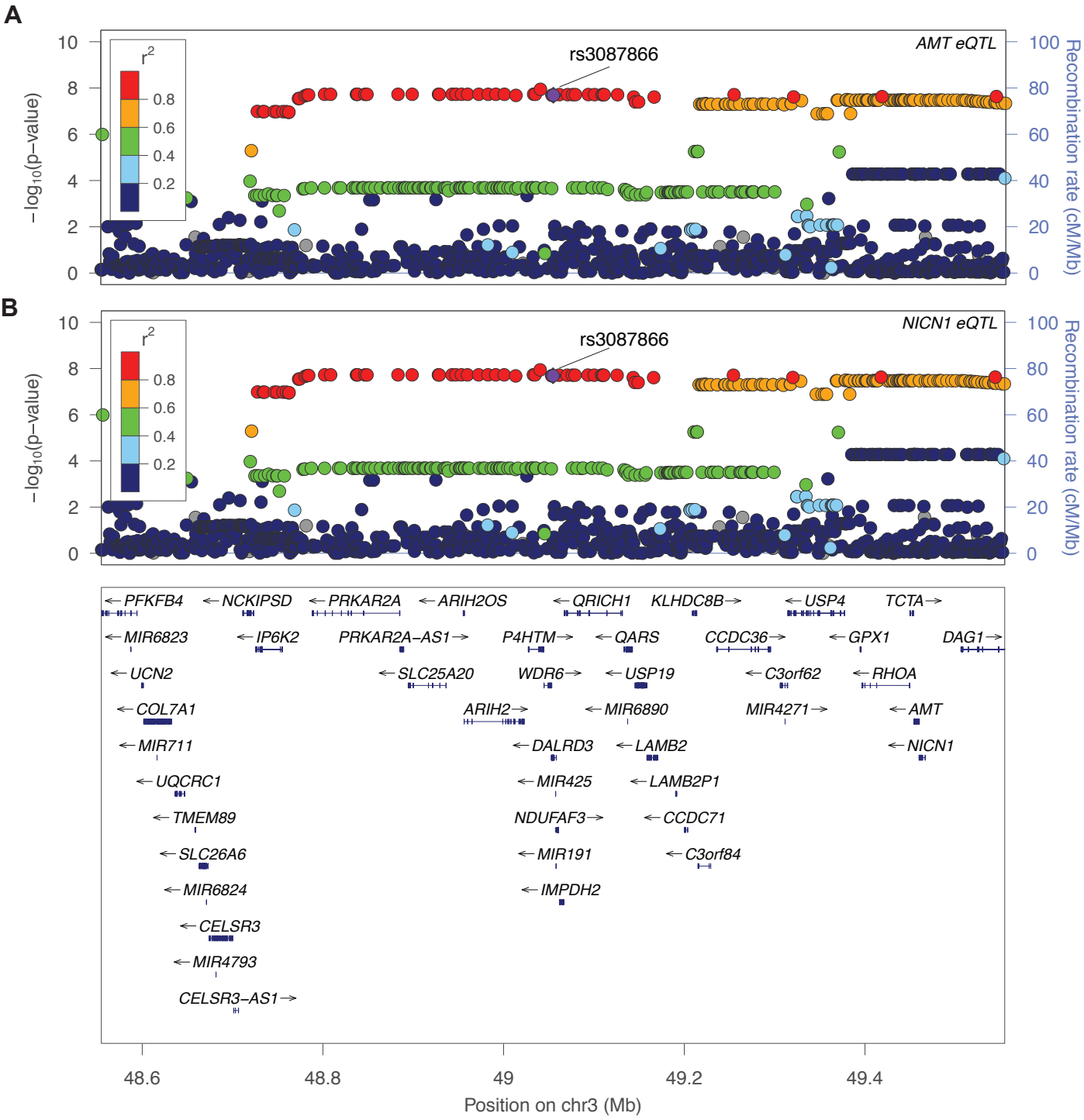

Figure S12. Subcutaneous adipose eQTLs for AMT and NICN1 colocalize with the DALRD3 novel adiponectin exome-wide locus. rs3087866 (purple diamond) shows the strongest association with adiponectin levels in the exome-wide meta-analysis at this locus). rs3087866 and 85 proxy variants (r^2>0.80; 1000Gp3) are nominally associated with adiponectin levels. The same variants exhibit the strongest association with expression of *AMT* (A) and *NICN1* (B) in subcutaneous adipose tissue. Each point represents a variant in the meta- or eQTL analysis, plotted with their P-value (on a -log10 scale) on the y-axis and genomic position (hg19) on the x-axis. The color of all other variants indicates the LD with the index variant in European ancestry haplotypes from the 1000 Genome Phase 3 reference panel. Based on eQTL colocalization with the adiponectin-associated variants, *AMT*, *NICN1*, and *PRKAR2A* are candidate genes at this locus.

Cohort Funding Information

The **Atherosclerosis Risk in Communities (ARIC)** study is carried out as a collaborative study supported by the National Heart, Lung, and Blood Institute (NHLBI) contracts (HHSN268201100005C, HHSN268201100006C, HHSN268201100007C, HHSN268201100008C, HHSN268201100009C, HHSN268201100010C, HHSN268201100011C, and HHSN268201100012C). The authors thank the staff and participants of the ARIC study for their important contributions. Funding support for "Building on GWAS for NHLBI-diseases: the U.S. CHARGE consortium" was provided by the NIH through the American Recovery and Reinvestment Act of 2009 (ARRA) (5RC2HL102419).

This **CHS** research was supported by NHLBI contracts HHSN268201200036C, HHSN268200800007C, HHSN268201800001C, N01HC55222, N01HC85079, N01HC85080, N01HC85081, N01HC85082, N01HC85083, N01HC85086; and NHLBI grants R01HL068986, U01HL080295, R01HL087652, R01HL105756, R01HL103612, R01HL120393, and U01HL130114 with additional contribution from the National Institute of Neurological Disorders and Stroke (NINDS). Additional support was provided through R01AG023629 from the National Institute on Aging (NIA). A full list of principal CHS investigators and institutions can be found at CHS-NHLBI.org. The provision of genotyping data was supported in part by the National Center for Advancing Translational Sciences, CTSI grant UL1TR000124, and the National Institute of Diabetes and Digestive and Kidney Disease Diabetes Research Center (DRC) grant DK063491 to the Southern California Diabetes Endocrinology Research Center. The content is solely the responsibility of the authors and does not necessarily represent the official views of the National Institutes of Health. Additional grant received from the AHA Clinically Applied Research Grant, R01 HL094555 from NHLBI.

CLHNS thanks the Office of Population Studies Foundation research and data collection teams and the study participants who generously provided their time for this study. This work was supported by National Institutes of Health grants DK078150, TW005596 and HL085144; pilot funds from RR020649, ES010126, and DK056350; and the Office of Population Studies Foundation.

The **Erasmus Rucphen Family** (**ERF)** study is grateful to all study participants and their relatives, general practitioners and neurologists for their contributions and to P. Veraart for her help in genealogy, J. Vergeer for the supervision of the laboratory work and P. Snijders for his help in data collection. ERF was supported by the Consortium for Systems Biology (NCSB), both within the framework of the Netherlands Genomics Initiative (NGI)/Netherlands Organisation for Scientific Research (NWO). ERF study as a part of EUROSPAN (European Special Populations Research Network) was supported by European Commission FP6 STRP grant number 018947 (LSHG-CT-2006-01947) and also received funding from the European Community's Seventh Framework Programme (FP7/2007-2013)/grant agreement HEALTH-F4-2007-201413 by the European Commission under the programme "Quality of Life and Management of the Living Resources" of 5th Framework Programme (no. QLG2-CT-2002-01254) as well as FP7 project EUROHEADPAIN (nr 602633). The ERF study was further supported by ENGAGE consortium and CMSB. High-throughput analysis of the ERF data was supported by joint grant from Netherlands Organization for Scientific Research and the Russian Foundation for Basic Research (NWO-RFBR 047.017.043)The exome-chip measurements have been funded by the Netherlands Organization for Scientific Research (NWO; project number 184021007) and by the Rainbow Project (RP10; Netherlands Exome Chip Project) of the Biobanking and Biomolecular Research Infrastructure Netherlands (BBMRI-NL; www.bbmri.nl (http://www.bbmri.nl)). Ayse Demirkan is supported by a Veni grant (2015) from ZonMw. Ayse Demirkan, Jun Liu and Cornelia van Duijn have used exchange grants from PRECEDI. The funders had no role in study design, data collection and analysis, decision to publish, or preparation of the manuscripts.

The **Fenland Study** is funded by the Wellcome Trust and the Medical Research Council (MC_U106179471). We are grateful to all the volunteers for their time and help, and to the General Practitioners and practice staff for assistance with recruitment. We thank the Fenland Study Investigators, Fenland Study Co-ordination team and the Epidemiology Field, Data and Laboratory teams. We further acknowledge support from the Medical research council (MC_UU_12015/1).

The **FINRISK07/DILGOM** is funded by the Academy of Finland (#118065 and #136895).

The **Framingham Heart Study** (FHS) was initiated in 1948 and is comprised of 5,209 participants from Framingham, MA (US), who have undergone examinations every other year to evaluate cardiovascular disease and related risk factors. The Offspring cohort was recruited in 1971 and includes 5,124 children of the Original cohort and the children's spouses[5]. Participants from the Offspring cohort have attended exams roughly every four years. Adiponectin levels were measured using specimens collected at the 7th exam from the Offspring cohort. The current analysis includes 2,223 individuals with available phenotypic and genotypic information.

The **Inter99** was initiated by Torben Jørgensen (PI), Knut Borch-Johnsen (co-PI), Hans Ibsen and Troels F. Thomsen. The steering committee comprises the former two and Charlotta Pisinger. The study was financially supported by research grants from the Danish Research Council, the Danish Centre for Health Technology Assessment, Novo Nordisk Inc., Research Foundation of Copenhagen County, Ministry of Internal Affairs and Health, the Danish Heart Foundation, the Danish Pharmaceutical Association, the Augustinus Foundation, the Ib Henriksen Foundation, the Becket Foundation, and the Danish Diabetes Association.

We thank the **Jackson Heart Study (JHS**) participants and staff for their contributions to this work. The JHS is supported by contracts HHSN268201300046C, HHSN268201300047C, HHSN268201300048C, HHSN268201300049C, HHSN268201300050C from the National Heart, Lung, and Blood Institute and the National Institute on Minority Health and Health Disparities.

The **KORA** research platform (KORA, Cooperative Research in the Region of Augsburg) was initiated and financed by the Helmholtz Zentrum München – German Research Center for Environmental Health, Neuherberg, Germany and supported by grants from the German Federal Ministry of Education and Research (BMBF), the Federal Ministry of Health (Berlin, Germany), the Ministry of Innovation, Science, Research and Technology of the state North Rhine-Westphalia (Düsseldorf, Germany), and the Munich Center of Health Sciences (MC Health) as part of LMUinnovativ. This research was supported by the European Union's Seventh Framework Programme (FP7-Health-F5-2012) under grant agreement no. 305280 (MIMOmics), by the Helmholtz-Russia Joint Research Group (HRJRG) 310, and by the German Center for Diabetes Research (DZD). We thank all members of field staffs who were involved in the planning and conduct of the MONICA/KORA Augsburg studies. The funders had no role in study design, data collection and analysis, decision to publish, or preparation of the manuscript.

Leipzig-Adults was supported by the Kompetenznetz Adipositas (Competence network for Obesity) funded by the Federal Ministry of Education and Research (German Obesity Biomaterial Bank; FKZ 01GI1128), and by grants from the Collaborative Research Center funded by the German Research Foundation (CRC 1052 "Obesity mechanisms"; B01, B03). IFB Adiposity Diseases is supported by the Federal Ministry of Education and Research (BMBF), Germany, FKZ: 01EO1501 (projects AD2-060E, AD2-06E95, AD2-06E99 to P.K.).

MESA was supported by the Multi-Ethnic Study of Atherosclerosis (MESA) contracts HHSN268201500003I, N01-HC-95159, N01-HC-95160, N01-HC-95161, N01-HC-95162, N01-HC-95163, N01-HC-95164, N01-HC-95165, N01-HC-95166, N01-HC-95167, N01-HC-95168, N01-HC-95169, UL1-TR-000040, UL1-TR-001079, and UL1-TR-001420. The provision of genotyping data was supported in part by the National Center for Advancing Translational Sciences, CTSI grant UL1TR001881, and the National Institute of Diabetes and Digestive and Kidney Disease Diabetes Research (DRC) grant DK063491.

METSIM was supported by Academy of Finland grants 77299, 124243, and 141226; the Finnish Heart Foundation; the Finnish Diabetes Foundation; the Juselius Foundation; the Commission of the European Community HEALTH-F2-2007-201681; National Institutes of Health grants R01DK093757, R01DK072193, U01DK105561, R01DK062370; National Human Genome Research Institute Division of Intramural Research project number Z01HG000024.

The authors of the **NEO study** thank all individuals who participated in the Netherlands Epidemiology in Obesity study, all participating general practitioners for inviting eligible participants and all research nurses for collection of the data. We thank the NEO study group, Pat van Beelen, Petra Noordijk and Ingeborg de Jonge for the coordination, lab and data management of the NEO study. The genotyping in the NEO study was supported by the Centre National de Génotypage (Paris, France), headed by Jean-Francois Deleuze. The NEO study is supported by the participating Departments, the Division and the Board of Directors of the Leiden University Medical Center, and by the Leiden University, Research Profile Area Vascular and Regenerative Medicine.

PIVUS/ULSAM studies were supported by Wellcome Trust Grants WT098017, WT064890, WT090532, Uppsala University, Uppsala University Hospital, the Swedish Research Council and the Swedish Heart-Lung Foundation.

The **RAINE study** was supported by the National Health and Medical Research Council of Australia [grant numbers 572613, 403981 and 003209] and the Canadian Institutes of Health Research [grant number MOP-82893]. The authors are grateful to the Raine Study participants and their families, and to the Raine Study research staff for cohort coordination and data collection. The authors gratefully acknowledge the NH&MRC for their long term contribution to funding the study over the last 29 years and also the following Institutions for providing funding for Core Management of the Raine Study: The University of Western Australia (UWA), Curtin University, Raine Medical Research Foundation, The Telethon Kids Institute, Women and Infants Research Foundation (King Edward Memorial Hospital), Murdoch University, The University of Notre Dame (Australia), and Edith Cowan University. The authors gratefully acknowledge the assistance of the Western Australian DNA Bank (National Health and Medical Research Council of Australia National Enabling Facility). This work was supported by resources provided by the Pawsey Supercomputing Centre with funding from the Australian Government and the Government of Western Australia.

The **RISC study** was supported by European Union grant QLG1-CT-2001-01252 and AstraZeneca. The initial genotyping of the RISC samples was funded by Merck & Co Inc.

RSI - The generation and management of the Illumina exome chip v1.0 array data for the Rotterdam Study (RS-I) was executed by the Human Genotyping Facility of the Genetic Laboratory of the Department of Internal Medicine, Erasmus MC, Rotterdam, The Netherlands. The Exome chip array data set was funded by the Genetic Laboratory of the Department of Internal Medicine, Erasmus MC, from

the Netherlands Genomics Initiative (NGI)/Netherlands Organisation for Scientific Research (NWO)-sponsored Netherlands Consortium for Healthy Aging (NCHA; project nr. 050-060-810); the Netherlands Organization for Scientific Research (NWO; project number 184021007) and by the Rainbow Project (RP10; Netherlands Exome Chip Project) of the Biobanking and Biomolecular Research Infrastructure Netherlands (BBMRI-NL; www.bbmri.nl). We thank Ms. Mila Jhamai, Ms. Sarah Higgins, and Mr. Marijn Verkerk for their help in creating the exome chip database, and Carolina Medina-Gomez, PhD , Lennard Karsten, MSc, and Linda Broer PhD for QC and variant calling. Variants were called using the best practice protocol developed by Grove et al. as part of the CHARGE consortium exome chip central calling effort. The Rotterdam Study is funded by Erasmus Medical Center and Erasmus University, Rotterdam, Netherlands Organization for the Health Research and Development (ZonMw), the Research Institute for Diseases in the Elderly (RIDE), the Ministry of Education, Culture and Science, the Ministry for Health, Welfare and Sports, the European Commission (DG XII), and the Municipality of Rotterdam. The authors are grateful to the study participants, the staff from the Rotterdam Study and the participating general practitioners and pharmacists. Additionally, the Netherlands Organization for Health Research and Development supported authors of this manuscript (C.M-G : ZonMw VIDI 016.136.367;).

Sorbs was supported by the Integrated Research and Treatment Center (IFB) Adiposity Diseases (K403, K737, AD2-7123). IFB is supported by the Federal Ministry of Education and Research (BMBF), Germany FKZ: 01EO1501. Sorbs was further supported by the German Research Foundation (CRC 1052 "Obesity mechanisms", A01; SPP 1629 TO 718/2-1) and by the German Diabetes Association.

TwinsUK is funded by the Wellcome Trust, Medical Research Council, European Union, the National Institute for Health Research (NIHR)-funded BioResource, Clinical Research Facility and Biomedical Research Centre based at Guy's and St Thomas' NHS Foundation Trust in partnership with King's College London.

The **WGHS** is supported by the National Heart, Lung, and Blood Institute (HL043851, HL080467, HL099355) and the National Cancer Institute (CA047988 and UM1CA182913) with collaborative scientific support and funding for genotyping provided by Amgen. Funding for leptin and adiponectin measures was provided by Roche.

The **Women's Health Initiative (WHI)** program is funded by the National Heart, Lung, and Blood Institute, National Institutes of Health, and the United States Department of Health and Human Services. Exome-chip data and analysis were supported through the Women's Health Initiative Sequencing Project (NHLBI RC2 HL-102924), the Genetics and Epidemiology of Colorectal Cancer Consortium (NCI CA137088), the Genomics and Randomized Trials Network (NHGRI U01-HG005152), and an NCI training grant (R25CA094880).

The **Young Finns Study** has been financially supported by the Academy of Finland: grants 286284, 134309 (Eye), 126925, 121584, 124282, 129378 (Salve), 117787 (Gendi), and 41071 (Skidi); the Social Insurance Institution of Finland; Competitive State Research Financing of the Expert Responsibility area of Kuopio, Tampere and Turku University Hospitals (grant X51001); Juho Vainio Foundation; Paavo Nurmi Foundation; Finnish Foundation for Cardiovascular Research ; Finnish Cultural Foundation; The Sigrid Juselius Foundation; Tampere Tuberculosis Foundation; Emil Aaltonen Foundation; Yrjö Jahnsson Foundation; Signe and Ane Gyllenberg Foundation; Diabetes Research Foundation of Finnish Diabetes Association; and EU Horizon 2020 (grant 755320 for TAXINOMISIS); and European Research Council (grant 742927 for MULTIEPIGEN project); Tampere University Hospital Supporting Foundation. We thank the teams that collected data at all measurement time points; the persons who participated as both

children and adults in these longitudinal studies; and biostatisticians Irina Lisinen, Johanna Ikonen, Noora Kartiosuo, Ville Aalto, and Jarno Kankaanranta for data management and statistical advice.

References

1. Andrieu, G., Quaranta, M., Leprince, C., and Hatzoglou, A. (2012). The GTPase Gem and its partner Kif9 are required for chromosome alignment, spindle length control, and mitotic progression. FASEB journal : official publication of the Federation of American Societies for Experimental Biology 26, 5025-5034.
2. Tikhonenko, I., Magidson, V., Graf, R., Khodjakov, A., and Koonce, M.P. (2013). A kinesin-mediated mechanism that couples centrosomes to nuclei. Cellular and molecular life sciences : CMLS 70, 1285-1296.
3. Fan, Y., Hanai, J.I., Le, P.T., Bi, R., Maridas, D., DeMambro, V., Figueroa, C.A., Kir, S., Zhou, X., Mannstadt, M., et al. (2017). Parathyroid Hormone Directs Bone Marrow Mesenchymal Cell Fate. Cell metabolism 25, 661-672.
4. Cawthorn, W.P., Scheller, E.L., Learman, B.S., Parlee, S.D., Simon, B.R., Mori, H., Ning, X., Bree, A.J., Schell, B., Broome, D.T., et al. (2014). Bone marrow adipose tissue is an endocrine organ that contributes to increased circulating adiponectin during caloric restriction. Cell metabolism 20, 368-375.
5. Tennenbaum, D.M., Manley, B.J., Zabor, E., Becerra, M.F., Carlo, M.I., Casuscelli, J., Redzematovic, A., Khan, N., Arcila, M.E., Voss, M.H., et al. (2017). Genomic alterations as predictors of survival among patients within a combined cohort with clear cell renal cell carcinoma undergoing cytoreductive nephrectomy. Urologic oncology 35, 532.e537-532.e513.
6. Chen, Z., Raghoonundun, C., Chen, W., Zhang, Y., Tang, W., Fan, X., and Shi, X. (2018). SETD2 indicates favourable prognosis in gastric cancer and suppresses cancer cell proliferation, migration, and invasion. Biochemical and biophysical research communications 498, 579-585.
7. Yuan, H., Li, N., Fu, D., Ren, J., Hui, J., Peng, J., Liu, Y., Qiu, T., Jiang, M., Pan, Q., et al. (2017). Histone methyltransferase SETD2 modulates alternative splicing to inhibit intestinal tumorigenesis. The Journal of clinical investigation 127, 3375-3391.
8. Husedzinovic, A., Neumann, B., Reymann, J., Draeger-Meurer, S., Chari, A., Erfle, H., Fischer, U., and Gruss, O.J. (2015). The catalytically inactive tyrosine phosphatase HD-PTP/PTPN23 is a novel regulator of SMN complex localization. Molecular biology of the cell 26, 161-171.
9. Smigiel, R., Landsberg, G., Schilling, M., Rydzanicz, M., Pollak, A., Walczak, A., Stodolak, A., Stawinski, P., Mierzewska, H., Sasiadek, M.M., et al. (2018). Developmental epileptic encephalopathy with hypomyelination and brain atrophy associated with PTPN23 variants affecting the assembly of UsnRNPs. European journal of human genetics : EJHG 26, 1502-1511.
10. Fan, C., Dong, L., Zhu, N., Xiong, Y., Zhang, J., Wang, L., Shen, Y., Zhang, X., and Chen, M. (2012). Isolation of siRNA target by biotinylated siRNA reveals that human CCDC12 promotes early erythroid differentiation. Leukemia research 36, 779-783.
11. London, E., Nesterova, M., Sinaii, N., Szarek, E., Chanturiya, T., Mastroyannis, S.A., Gavrilova, O., and Stratakis, C.A. (2014). Differentially regulated protein kinase A (PKA) activity in adipose tissue and liver is associated with resistance to diet-induced obesity and glucose intolerance in mice that lack PKA regulatory subunit type IIalpha. Endocrinology 155, 3397-3408.
12. Applegarth, D.A., and Toone, J.R. (2001). Nonketotic hyperglycinemia (glycine encephalopathy): laboratory diagnosis. Molecular genetics and metabolism 74, 139-146.
13. Ververi, A., Splitt, M., Dean, J.C.S., and Brady, A.F. (2018). Phenotypic spectrum associated with de novo mutations in QRICH1 gene. Clinical genetics 93, 286-292.
14. Pierre, G., Macdonald, A., Gray, G., Hendriksz, C., Preece, M.A., and Chakrapani, A. (2007). Prospective treatment in carnitine-acylcarnitine translocase deficiency. Journal of inherited metabolic disease 30, 815.

15. Lim, K.H., Choi, J.H., Park, J.H., Cho, H.J., Park, J.J., Lee, E.J., Li, L., Choi, Y.K., and Baek, K.H. (2016). Ubiquitin specific protease 19 involved in transcriptional repression of retinoic acid receptor by stabilizing CORO2A. Oncotarget 7, 34759-34772.
16. Bedard, N., Jammoul, S., Moore, T., Wykes, L., Hallauer, P.L., Hastings, K.E., Stretch, C., Baracos, V., Chevalier, S., Plourde, M., et al. (2015). Inactivation of the ubiquitin-specific protease 19 deubiquitinating enzyme protects against muscle wasting. FASEB journal : official publication of the Federation of American Societies for Experimental Biology 29, 3889-3898.
17. Zheng, B., Ma, Y.C., Ostrom, R.S., Lavoie, C., Gill, G.N., Insel, P.A., Huang, X.Y., and Farquhar, M.G. (2001). RGS-PX1, a GAP for GalphaS and sorting nexin in vesicular trafficking. Science (New York, NY) 294, 1939-1942.
18. Mas, C., Norwood, S.J., Bugarcic, A., Kinna, G., Leneva, N., Kovtun, O., Ghai, R., Ona Yanez, L.E., Davis, J.L., Teasdale, R.D., et al. (2014). Structural basis for different phosphoinositide specificities of the PX domains of sorting nexins regulating G-protein signaling. The Journal of biological chemistry 289, 28554-28568.
19. Chatterjee, T.K., Idelman, G., Blanco, V., Blomkalns, A.L., Piegore, M.G., Jr., Weintraub, D.S., Kumar, S., Rajsheker, S., Manka, D., Rudich, S.M., et al. (2011). Histone deacetylase 9 is a negative regulator of adipogenic differentiation. The Journal of biological chemistry 286, 27836-27847.
20. Chatterjee, T.K., Basford, J.E., Knoll, E., Tong, W.S., Blanco, V., Blomkalns, A.L., Rudich, S., Lentsch, A.B., Hui, D.Y., and Weintraub, N.L. (2014). HDAC9 knockout mice are protected from adipose tissue dysfunction and systemic metabolic disease during high-fat feeding. Diabetes 63, 176-187.
21. Schwefel, D., Arasu, B.S., Marino, S.F., Lamprecht, B., Kochert, K., Rosenbaum, E., Eichhorst, J., Wiesner, B., Behlke, J., Rocks, O., et al. (2013). Structural insights into the mechanism of GTPase activation in the GIMAP family. Structure (London, England : 1993) 21, 550-559.
22. Astle, W.J., Elding, H., Jiang, T., Allen, D., Ruklisa, D., Mann, A.L., Mead, D., Bouman, H., Riveros-Mckay, F., Kostadima, M.A., et al. (2016). The Allelic Landscape of Human Blood Cell Trait Variation and Links to Common Complex Disease. Cell 167, 1415-1429.e1419.
23. Houchens, C.R., Montigny, W., Zeltser, L., Dailey, L., Gilbert, J.M., and Heintz, N.H. (2000). The dhfr oribeta-binding protein RIP60 contains 15 zinc fingers: DNA binding and looping by the central three fingers and an associated proline-rich region. Nucleic acids research 28, 570-581.
24. Ruschke, K., Illes, M., Kern, M., Kloting, I., Fasshauer, M., Schon, M.R., Kosacka, J., Fitzl, G., Kovacs, P., Stumvoll, M., et al. (2010). Repin1 maybe involved in the regulation of cell size and glucose transport in adipocytes. Biochemical and biophysical research communications 400, 246-251.
25. Kunath, A., Hesselbarth, N., Gericke, M., Kern, M., Dommel, S., Kovacs, P., Stumvoll, M., Bluher, M., and Kloting, N. (2016). Repin1 deficiency improves insulin sensitivity and glucose metabolism in db/db mice by reducing adipose tissue mass and inflammation. Biochemical and biophysical research communications 478, 398-402.
26. Helfer, G., and Wu, Q.F. (2018). Chemerin: a multifaceted adipokine involved in metabolic disorders. The Journal of endocrinology 238, R79-r94.
27. Goralski, K.B., McCarthy, T.C., Hanniman, E.A., Zabel, B.A., Butcher, E.C., Parlee, S.D., Muruganandan, S., and Sinal, C.J. (2007). Chemerin, a novel adipokine that regulates adipogenesis and adipocyte metabolism. The Journal of biological chemistry 282, 28175-28188.
28. Condamine, T., Le Texier, L., Howie, D., Lavault, A., Hill, M., Halary, F., Cobbold, S., Waldmann, H., Cuturi, M.C., and Chiffoleau, E. (2010). Tmem176B and Tmem176A are associated with the immature state of dendritic cells. Journal of leukocyte biology 88, 507-515.
29. Kirschner, K.M., Braun, J.F., Jacobi, C.L., Rudigier, L.J., Persson, A.B., and Scholz, H. (2014). Amine oxidase copper-containing 1 (AOC1) is a downstream target gene of the Wilms tumor protein, WT1, during kidney development. The Journal of biological chemistry 289, 24452-24462.

30. Sass, J.O., Gemperle-Britschgi, C., Tarailo-Graovac, M., Patel, N., Walter, M., Jordanova, A., Alfadhel, M., Baric, I., Coker, M., Damli-Huber, A., et al. (2016). Unravelling 5-oxoprolinuria (pyroglutamic aciduria) due to bi-allelic OPLAH mutations: 20 new mutations in 14 families. Molecular genetics and metabolism 119, 44-49.
31. Rideout, E.J., Marshall, L., and Grewal, S.S. (2012). Drosophila RNA polymerase III repressor Maf1 controls body size and developmental timing by modulating tRNAiMet synthesis and systemic insulin signaling. Proceedings of the National Academy of Sciences of the United States of America 109, 1139-1144.
32. Khanna, A., Johnson, D.L., and Curran, S.P. (2014). Physiological roles for mafr-1 in reproduction and lipid homeostasis. Cell reports 9, 2180-2191.
33. Willis, I.M. (2018). Maf1 phenotypes and cell physiology. Biochimica et biophysica acta Gene regulatory mechanisms 1861, 330-337.
34. Palian, B.M., Rohira, A.D., Johnson, S.A., He, L., Zheng, N., Dubeau, L., Stiles, B.L., and Johnson, D.L. (2014). Maf1 is a novel target of PTEN and PI3K signaling that negatively regulates oncogenesis and lipid metabolism. PLoS genetics 10, e1004789.
35. Khanna, A., Pradhan, A., and Curran, S.P. (2015). Emerging Roles for Maf1 beyond the Regulation of RNA Polymerase III Activity. Journal of molecular biology 427, 2577-2585.
36. Poulter, J.A., Al-Araimi, M., Conte, I., van Genderen, M.M., Sheridan, E., Carr, I.M., Parry, D.A., Shires, M., Carrella, S., Bradbury, J., et al. (2013). Recessive mutations in SLC38A8 cause foveal hypoplasia and optic nerve misrouting without albinism. American journal of human genetics 93, 1143-1150.
37. Yamauchi, T., Kamon, J., Ito, Y., Tsuchida, A., Yokomizo, T., Kita, S., Sugiyama, T., Miyagishi, M., Hara, K., Tsunoda, M., et al. (2003). Cloning of adiponectin receptors that mediate antidiabetic metabolic effects. Nature 423, 762-769.
38. Hug, C., Wang, J., Ahmad, N.S., Bogan, J.S., Tsao, T.S., and Lodish, H.F. (2004). T-cadherin is a receptor for hexameric and high-molecular-weight forms of Acrp30/adiponectin. Proceedings of the National Academy of Sciences of the United States of America 101, 10308-10313.
39. Sakai, J., Rawson, R.B., Espenshade, P.J., Cheng, D., Seegmiller, A.C., Goldstein, J.L., and Brown, M.S. (1998). Molecular identification of the sterol-regulated luminal protease that cleaves SREBPs and controls lipid composition of animal cells. Molecular cell 2, 505-514.
40. Ramos-Lopez, O., Riezu-Boj, J.I., Milagro, F.I., and Martinez, J.A. (2018). DNA methylation signatures at endoplasmic reticulum stress genes are associated with adiposity and insulin resistance. Molecular genetics and metabolism 123, 50-58.
41. Lundback, V., Kulyte, A., Strawbridge, R.J., Ryden, M., Arner, P., Marcus, C., and Dahlman, I. (2018). FAM13A and POM121C are candidate genes for fasting insulin: functional follow-up analysis of a genome-wide association study. Diabetologia 61, 1112-1123.
42. Wardhana, D.A., Ikeda, K., Barinda, A.J., Nugroho, D.B., Qurania, K.R., Yagi, K., Miyata, K., Oike, Y., Hirata, K.I., and Emoto, N. (2018). Family with sequence similarity 13, member A modulates adipocyte insulin signaling and preserves systemic metabolic homeostasis. Proceedings of the National Academy of Sciences of the United States of America 115, 1529-1534.
43. He, L., Girijashanker, K., Dalton, T.P., Reed, J., Li, H., Soleimani, M., and Nebert, D.W. (2006). ZIP8, member of the solute-carrier-39 (SLC39) metal-transporter family: characterization of transporter properties. Molecular pharmacology 70, 171-180.
44. Zhang, R., Witkowska, K., Afonso Guerra-Assuncao, J., Ren, M., Ng, F.L., Mauro, C., Tucker, A.T., Caulfield, M.J., and Ye, S. (2016). A blood pressure-associated variant of the SLC39A8 gene influences cellular cadmium accumulation and toxicity. Human molecular genetics 25, 4117-4126.

45. Lin, W., Vann, D.R., Doulias, P.T., Wang, T., Landesberg, G., Li, X., Ricciotti, E., Scalia, R., He, M., Hand, N.J., et al. (2017). Hepatic metal ion transporter ZIP8 regulates manganese homeostasis and manganese-dependent enzyme activity. The Journal of clinical investigation 127, 2407-2417.
46. Boycott, K.M., Beaulieu, C.L., Kernohan, K.D., Gebril, O.H., Mhanni, A., Chudley, A.E., Redl, D., Qin, W., Hampson, S., Kury, S., et al. (2015). Autosomal-Recessive Intellectual Disability with Cerebellar Atrophy Syndrome Caused by Mutation of the Manganese and Zinc Transporter Gene SLC39A8. American journal of human genetics 97, 886-893.
47. Pickrell, J.K., Berisa, T., Liu, J.Z., Segurel, L., Tung, J.Y., and Hinds, D.A. (2016). Detection and interpretation of shared genetic influences on 42 human traits. Nature genetics 48, 709-717.
48. Nagai, Y., Nishimura, A., Tago, K., Mizuno, N., and Itoh, H. (2010). Ric-8B stabilizes the alpha subunit of stimulatory G protein by inhibiting its ubiquitination. The Journal of biological chemistry 285, 11114-11120.
49. Maureira, A., Sanchez, R., Valenzuela, N., Torrejon, M., Hinrichs, M.V., Olate, J., and Gutierrez, J.L. (2016). The CREB Transcription Factor Controls Transcriptional Activity of the Human RIC8B Gene. Journal of cellular biochemistry 117, 1797-1805.
50. Griebel, G., Ravinet-Trillou, C., Beeske, S., Avenet, P., and Pichat, P. (2014). Mice deficient in cryptochrome 1 (cry1 (-/-)) exhibit resistance to obesity induced by a high-fat diet. Frontiers in endocrinology 5, 49.
51. Jang, H., Lee, G.Y., Selby, C.P., Lee, G., Jeon, Y.G., Lee, J.H., Cheng, K.K., Titchenell, P., Birnbaum, M.J., Xu, A., et al. (2016). SREBP1c-CRY1 signalling represses hepatic glucose production by promoting FOXO1 degradation during refeeding. Nat Commun 7, 12180.
52. Calabrese, G.M., Mesner, L.D., Stains, J.P., Tommasini, S.M., Horowitz, M.C., Rosen, C.J., and Farber, C.R. (2017). Integrating GWAS and Co-expression Network Data Identifies Bone Mineral Density Genes SPTBN1 and MARK3 and an Osteoblast Functional Module. Cell systems 4, 46-59.e44.
53. Hyvarinen, A.K., Pohjoismaki, J.L., Holt, I.J., and Jacobs, H.T. (2011). Overexpression of MTERFD1 or MTERFD3 impairs the completion of mitochondrial DNA replication. Molecular biology reports 38, 1321-1328.
54. Manenschijn, L., van den Akker, E.L., Lamberts, S.W., and van Rossum, E.F. (2009). Clinical features associated with glucocorticoid receptor polymorphisms. An overview. Annals of the New York Academy of Sciences 1179, 179-198.
55. Peckett, A.J., Wright, D.C., and Riddell, M.C. (2011). The effects of glucocorticoids on adipose tissue lipid metabolism. Metabolism: clinical and experimental 60, 1500-1510.
56. Ferrau, F., and Korbonits, M. (2015). Metabolic comorbidities in Cushing's syndrome. European journal of endocrinology / European Federation of Endocrine Societies 173, M133-157.
57. Lee, M.J., and Fried, S.K. (2014). The glucocorticoid receptor, not the mineralocorticoid receptor, plays the dominant role in adipogenesis and adipokine production in human adipocytes. International journal of obesity (2005) 38, 1228-1233.
58. Pantoja, C., Huff, J.T., and Yamamoto, K.R. (2008). Glucocorticoid signaling defines a novel commitment state during adipogenesis in vitro. Molecular biology of the cell 19, 4032-4041.
59. Shen, Y., Roh, H.C., Kumari, M., and Rosen, E.D. (2017). Adipocyte glucocorticoid receptor is important in lipolysis and insulin resistance due to exogenous steroids, but not insulin resistance caused by high fat feeding. Molecular metabolism 6, 1150-1160.
60. Estep, P.W., 3rd, Warner, J.B., and Bulyk, M.L. (2009). Short-term calorie restriction in male mice feminizes gene expression and alters key regulators of conserved aging regulatory pathways. PloS one 4, e5242.
61. Chu, A.Y., Deng, X., Fisher, V.A., Drong, A., Zhang, Y., Feitosa, M.F., Liu, C.T., Weeks, O., Choh, A.C., Duan, Q., et al. (2017). Multiethnic genome-wide meta-analysis of ectopic fat depots identifies loci associated with adipocyte development and differentiation. Nature genetics 49, 125-130.